In-situ Optical Monitoring of Operating Gas Turbine Blade Coatings Under Extreme Environments

DE-FE0031282

Fossil Energy Sensor & Control Project Review Meeting

Quentin Fouliard, Post-doctoral Fellow

PI: Seetha Raghavan, Co-PI: Ranajay Ghosh

https://aerostructures.cecs.ucf.edu/

May 19, 2021

Key goals

- Develop and demonstrate at the laboratory scale an advanced optical suite of instrumentation technologies for enhanced monitoring of gas turbine thermal barrier coatings (TBCs)
- **One-year extension assigned for the demonstration of surface temperature measurement capability and deployment of the instrumentation on an engine rig for in-situ phosphor thermometry**

Project Tasks **(Tasks 1-5: Oct 2017 – Oct 2020, + Task 6: Oct 2020 – Oct 2021)**

Task 1: Project Management & Planning
Task 2: Define and manufacture sensor configuration
Task 3: Establish Sensing Properties and Characterize Coating Response for Luminescence Based Sensor
Task 4: Perform Non-Intrusive Benchmarking Measurements of Surface Temperature and Strain
Task 5: Develop and Test Laboratory Scale Sensor Instrumentation Package
Task 6: Instrumentation adaptation to engine rig + surface measurements

Overview of the presentation

- **Background, Motivations & Objectives**
  - Thermal Barrier Coatings and their benefits

- **Research effort was focused on providing solutions for the following:**
  - **Higher accuracy of temperature measurements (part A)**
    - **Phosphor Thermometry experimentation**
  - **Improving methods for coating damage monitoring (part B)**
    - **Coating damage monitoring**

- **Conclusions and perspectives**

Background, Motivations & Objectives

Thermal Barrier Coatings (TBCs)

- **Thermal barrier coatings (TBCs)** used in combination with air cooling to protect metal substrates from extreme temperatures in the high-pressure turbine (1300 to 1600°C)

  Clarke, D (2012). *MRS Bulletin*, 37(10), 891-898

  - Air film cooling: ΔT= -100 to -400°C

    Kotowicz, J, et al. *Archives of Thermodynamics* 37.4 (2016): 19-35

  - **TBC: ΔT= -150 to -200°C [3,4,5,6]**

    Sobhanverdi, R. and Alireza A. *Ceramics International* 41.10 (2015): 14517-14528.
    Bacos, M. P., et al. *Review of ONERA Activities* (2011).
    Darolia, R. *International Materials Reviews* 58.6 (2013): 315-348.
    Xu, Li, et al. *Procedia Engineering* 99 (2015): 1482-1491.

- **Major applications:**
  - Aeroengines
  - Power generation engines

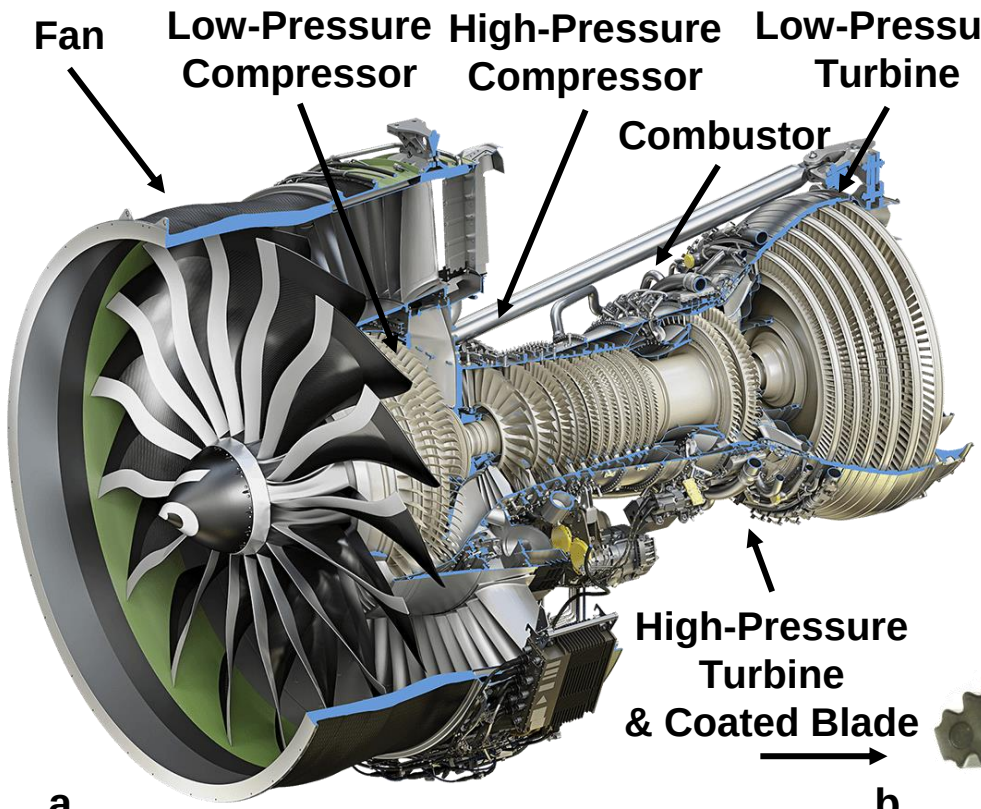

Darolia, R. *International Materials Reviews* 58.6 (2013): 315-348.

Image source: GE

Image source: GE

a) Cutaway view of the new GE9X aircraft engine
b) Photograph of a turbine blade coated with TBC
c) SEM micrograph of an EB-PVD TBC top coat

Review of TBC materials properties

TBC layer Typical composition	**Top coat** **7-8wt.%YSZ**	**TGO** **Al_2O_3**	**Bond coat** **NiCrAlY / PtAl**
Thermal conductivity λ at 1100°C (W/(m·K))	**1-3** [1,2,4,5]	**5-6** [4,6]	**34** [5]
Coefficient of thermal expansion α ($\times 10^{-6}$ K^{-1})	**11-13** [3,4,7,8]	**7-10** [3,7,8,9]	**13-16** [3,7,8,9]
Elastic modulus (GPa)	**0-100** [13]	**320-434** [3,7,8,9]	**110-240** [3,7,9]
Toughness K (MPa· $\sqrt{m}$)	**0.7-2.2** [7,10]	**2.8-3.2** [7,11]	**>20** [7]
Poisson's ratio ν	**0.2** [8]	**0.2-0.25** [8,9]	**0.3-0.33** [8,9]
Oxygen diffusivity at 1000°C (m^2/s)	**10^{-11}** [4]	**10^{-19}-10^{-21}** [4,6]	-
Crystal microstructure (phase) Stable up to	t' **1200°C** [12]	α **1750°C**	β, γ **1050°C**

[14]

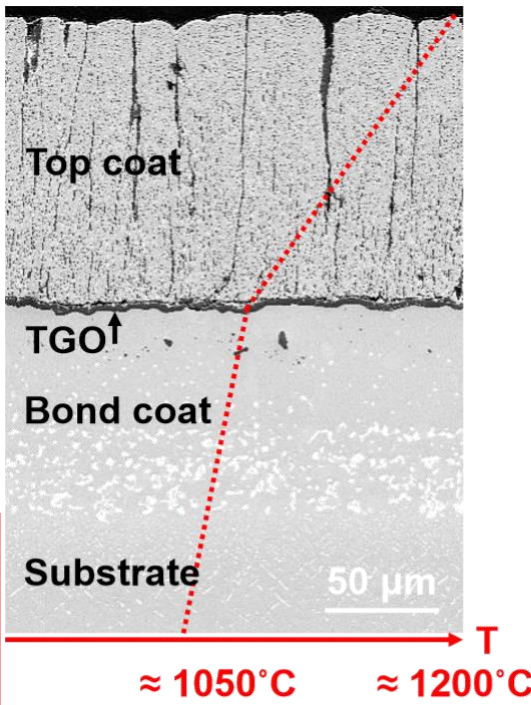

[1] Dinwiddie, Ralph B., et al. No. CONF-9606158-1. Oak Ridge National Lab., TN, USA, 1996
[2] Nicholls, John R., et al. *Surface and Coatings Technology* 151 (2002): 383-391.
[3] Liu, Jing., *PhD dissertation University of Central Florida* (2007).
[4] Lee, Woo Y., et al. *Journal of the American Ceramic Society* 79.12 (1996): 3003-3012.
[5] Lim, Geunsik, and Aravinda Kar. *Journal of Physics D: Applied Physics* 42.15 (2009): 155412.
[6] Steenbakker, Remy. *PhD dissertation Cranfield University*, (2008).
[7] Rabiei, et al. *Acta materialia* 48.15 (2000): 3963-3976.
[8] Yang, Lixia, et al. *Surface and Coatings Technology* 251 (2014): 98-105.
[9] Busso, E., et al. *Acta materialia* 55.5 (2007): 1491-1503.
[10] Liu, Y. et al. *Surface and Coatings Technology* 313 (2017): 417-424.
[11] Petit, J. *PhD dissertation University Pierre été Marie Curie – Paris VI* (2006).
[12] Witz, G., et al. *Advanced Ceramic Coatings and Interfaces II: Ceramic and Engineering Science Proceedings, Volume 28, Issue 3* (2007): 39-51.
[13] Renusch, D., et al. *Materials and corrosion* 59.7 (2008): 547-555.
[14] Fouliard, Q. *PhD dissertation University of Central Florida* (2019).

Thermally grown oxide (TGO) formation in TBCs

Importance of controlling the operating temperature

- **Logarithmic growth limited by the low oxygen diffusivity through the TGO:**

$$3\beta NiAl + \frac{3}{2}O_2 \rightarrow \gamma' Ni_3Al + \alpha Al_2O_3$$

Liu, Y. Z., et al. *Journal of the European Ceramic Society* 36.7 (2016): 1765-1774.
Bernard, B., *PhD dissertation, Université de Lorraine* (2016)

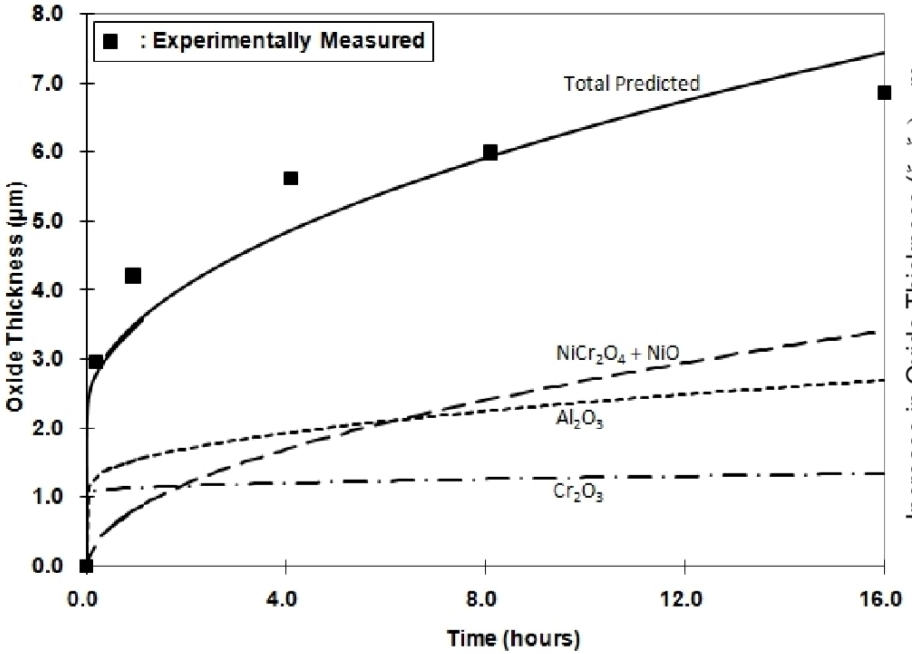

Wu, B, et al. *Journal of the American Ceramic Society* 72.2 (1989): 212-218.

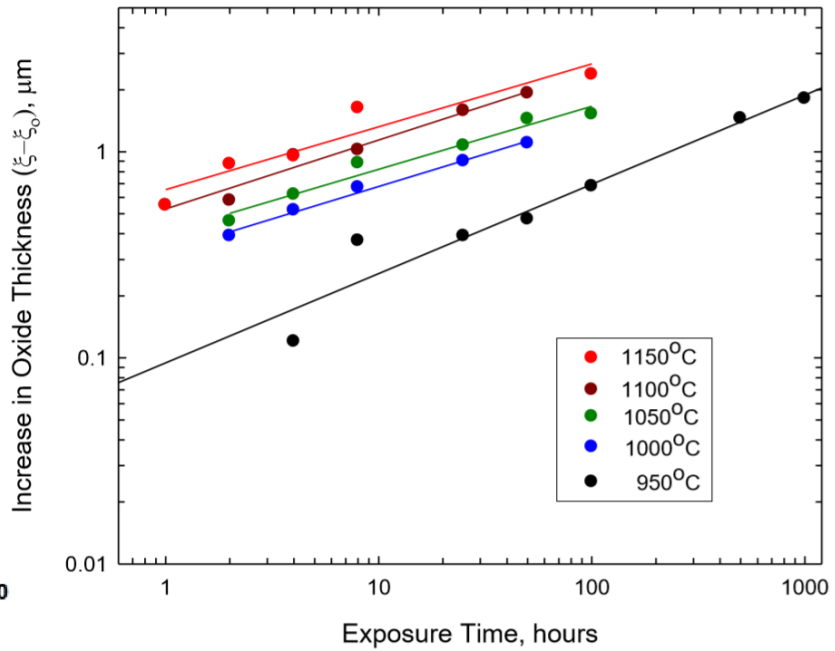

Jackson, R, *PhD dissertation University of Birmingham* (2009)

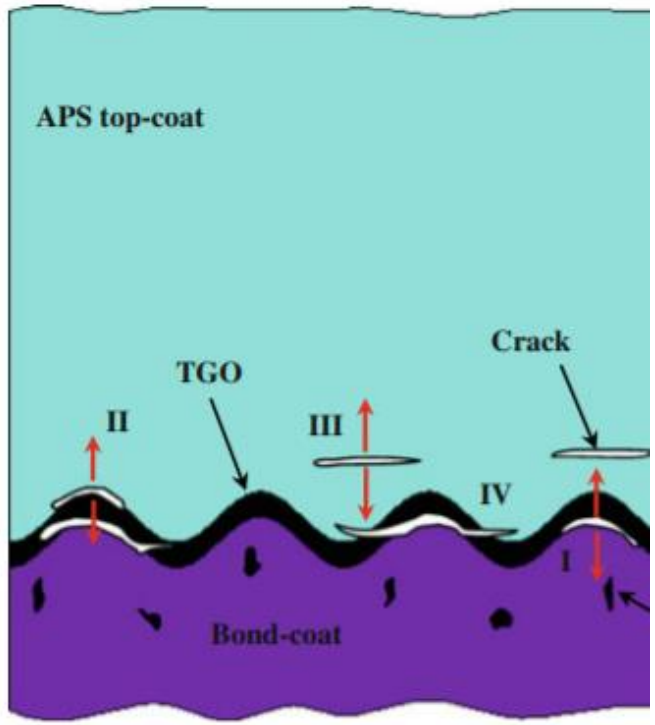

Wang, L., et al *Journal of thermal spray technology* 23.3 (2014): 431-446.

Temperature drives oxide growth in TBCs and is a key factor in coating failure

Phase stability in Thermal Barrier Coatings (TBCs)

Importance of controlling the operating temperature

- **Standard top coat material**: 7-8wt.% (4-4.5 mol.%) YSZ optimal for resistance to spallation and thermal stability Patnaik, P. et al, National Research Council Of Canada Ottawa, Ontario (2006)
  - **Y^{3+} introduces oxygen vacancies that stabilizes t'**

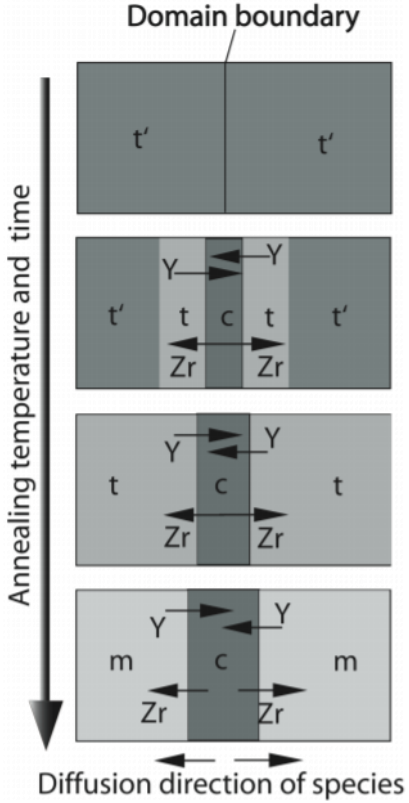

Witz, G., et al. *Advanced Ceramic Coatings and Interfaces II: Ceramic and Engineering Science Proceedings, Volume 28, Issue 3* (2007): 39-51.

  - **High temperature sintering of t'-YSZ:**
    - **Pore coarsening → thermal conductivity increase** Guignard, A. *Vol. 141. Forschungszentrum*, Jülich, (2012).
    - **Crack forming**
  - **t' phase stable up to 1200°C:**
  - $$t' \xrightarrow[1200°C]{} t + c \xrightarrow[600°C]{} m + c$$
    $$\Delta V = +4\%$$

Accurate control of TBC operating temperature is needed to control degradation of coatings.

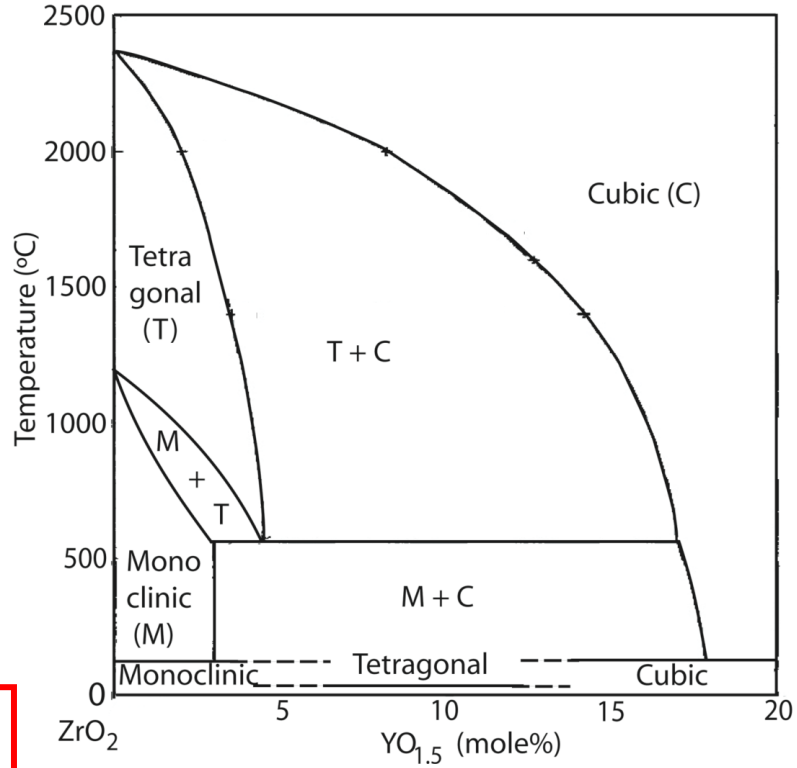

Witz, G., et al. *Advanced Ceramic Coatings and Interfaces II: Ceramic and Engineering Science Proceedings, Volume 28, Issue 3* (2007): 39-51.

Significance of TBC temperature measurements

- State-of-the-art TBCs are not being used to their highest potential because of uncertainties in temperature measurements at high-temperature.
  - Safety margins as high as 200°C are used.

Steenbakker, R, (2009) *Journal of Engineering for Gas Turbine and Power*, 131-4 p 041301

- Ideal Brayton cycle efficiency: $\eta = 1 - \frac{T_c}{T_t}$

η: cycle efficiency, $\frac{T_c}{T_t}$: temperature ratio compressor exit / turbine inlet.

- 1% efficiency improvement can save $20m in fuel over the combined-cycle plant life.
- A 130°C increase leads to a 4% increase in engine efficiency.

Ruud, J, (2003). *Performance of the Third*, 50 pp 950-4.

- Failure mechanisms are driven by temperature conditions in the depth of the TBC.

Problem statement:

Accurate determination of thermal gradients in Thermal Barrier Coatings (TBCs) is critical for the safe and efficient operation of gas turbine engines.
Failure mechanisms are thermally activated during engine operation, uncertainty in temperature measurements contribute significantly to lifetime uncertainty.

Measurement techniques for *in-situ* temperature evaluation of TBCs

	Thermocouples	Infrared Thermometry	Phosphor Thermometry
Operational temperature range (˚C)	-250 to 2320	-50 to 2000	-250 to 1700
Advantages	- Inexpensive - Wide temperature range	- Wide temperature range - Non-contact method - Fast response time	- **Non-contact method** - **High sensitivity at high temperatures** - **Fast response time** - **Usable on rotating parts** - **Low sensitivity to turbine environment (aging and contamination)**
Drawbacks	- Intrusive probe - Disrupts flow patterns - Not chemically stable in all environments - Low accuracy - Unusable on rotating surfaces	- Optical access required - Sensitive to stray light (flames) - Sensitive to emissivity variations	- Optical access required - Signal weakening at high temperatures

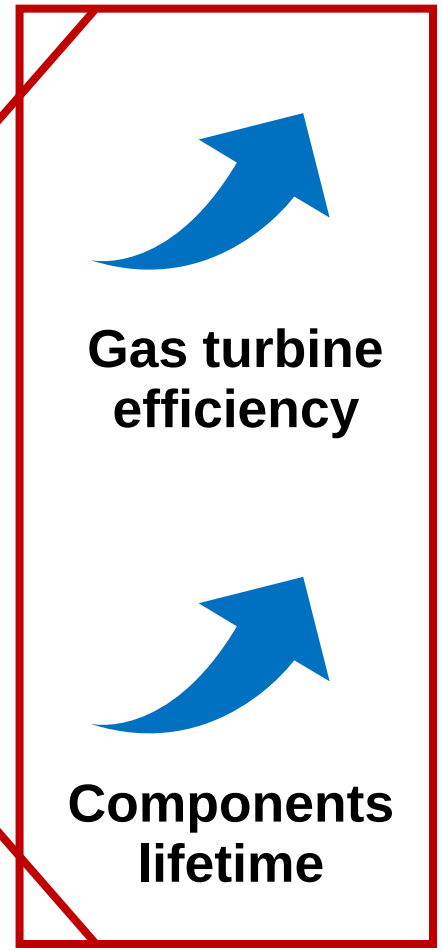

Other critical failure mechanisms: Foreign object damage / Erosion

Importance of controlling coating health

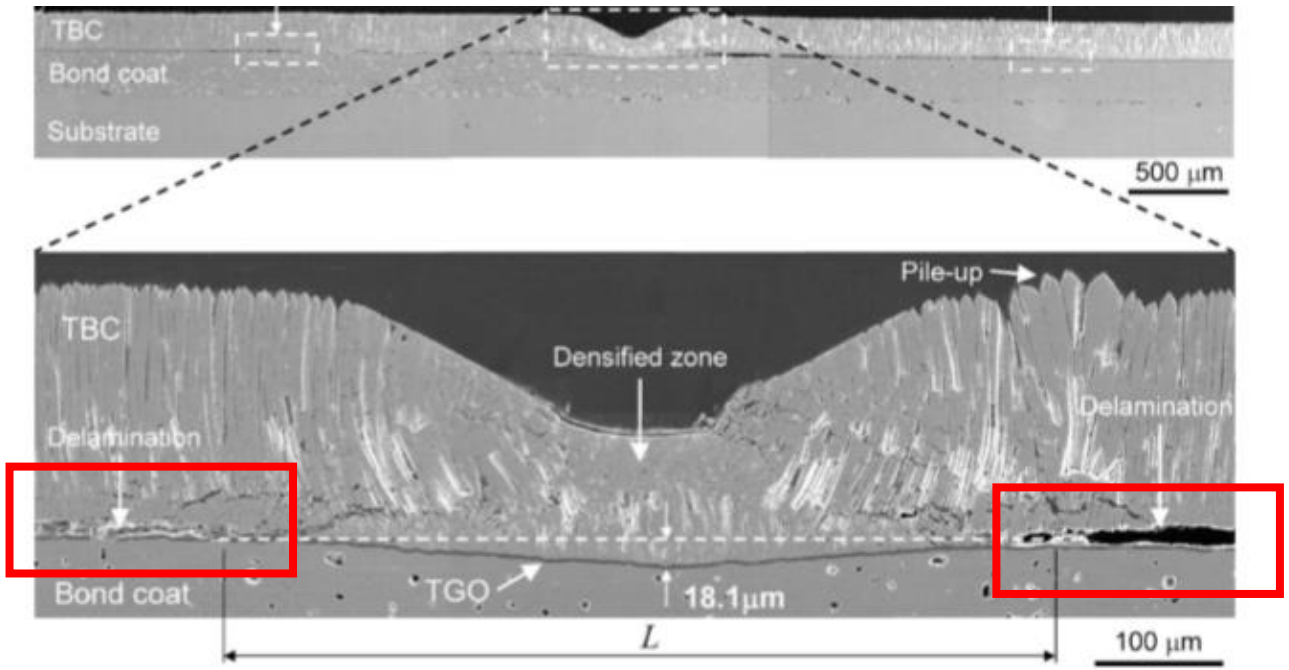

Tanaka, Makoto, Yu-Fu Liu, and Yutaka Kagawa. *Journal of Materials Research* 24.12 (2009): 3533-3542.

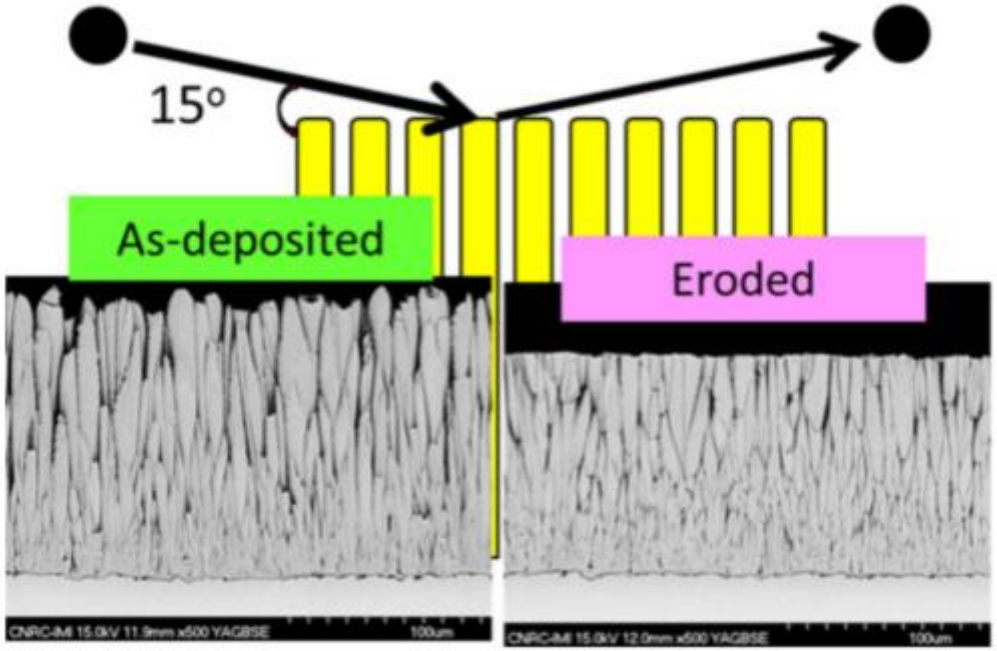

Lima, Rogerio S., Bruno MH Guerreiro, and Maniya Aghasibeig. *Journal of Thermal Spray Technology* 28.1-2 (2019): 223-232.

- Unpredictability of the impact damage/erosion
- Amount of degradation

  → **Importance of improving methods for detection and quantification of delamination**

Direct damage monitoring methods

- Thermal/optical imaging techniques;
  - Infrared thermography in mid-wave or long-wave infrared, post-exposition to an intense heat source (generally a flash of light).
  - Tomography
  - Laser scattering
  - Luminescence-based mapping (in-situ or ex-situ monitoring), under excitation at specific wavelength.

Luminescence imaging provides:

- **Finer spatial resolution**
- **Richer information through spectral features**

Proposed solutions & key objectives

- **Better temperature control in gas turbine engines is needed to improve engine efficiency and reduce maintenance and operation costs (part A)**

→ Implementation of phosphor thermometry instrumentation with accuracy/precision improvement vs. current state-of-the-art

→ Determination of precise sub-surface location of phosphor thermometry measurement point

- **Intense operation of TBC systems results in coating failure that impacts engine availability (parts B and C)**

→ Development of a novel approach for delamination monitoring using luminescent coatings (compatible with phosphor thermometry coatings)

→ Verification of sensor coating properties in operational environments

Part A: Phosphor Thermometry measurements

Part of tasks 2, 3, 4, 5 & 6

Phosphor Thermometry – fundamentals

- Typical dopants are rare-earth elements and transition metals.
- Electronic configuration determines the usable excitation wavelength.
- Emission wavelength is generally longer than excitation wavelength.

Brübach et al., *Progress in Energy and Combustion Science* (2013) 39(1), pp. 37-60
Chambers, M., and Clarke, D. *Annual Review of Materials Research* 39 (2009): 325-359.
Allison, S. and Gillies, G. *Review of Scientific Instruments* 68.7 (1997): 2615-2650.
Feist, J., et al. *Proceedings of the Institution of Mechanical Engineers, Part A: Journal of Power and Energy* 217.2 (2003): 193-200.

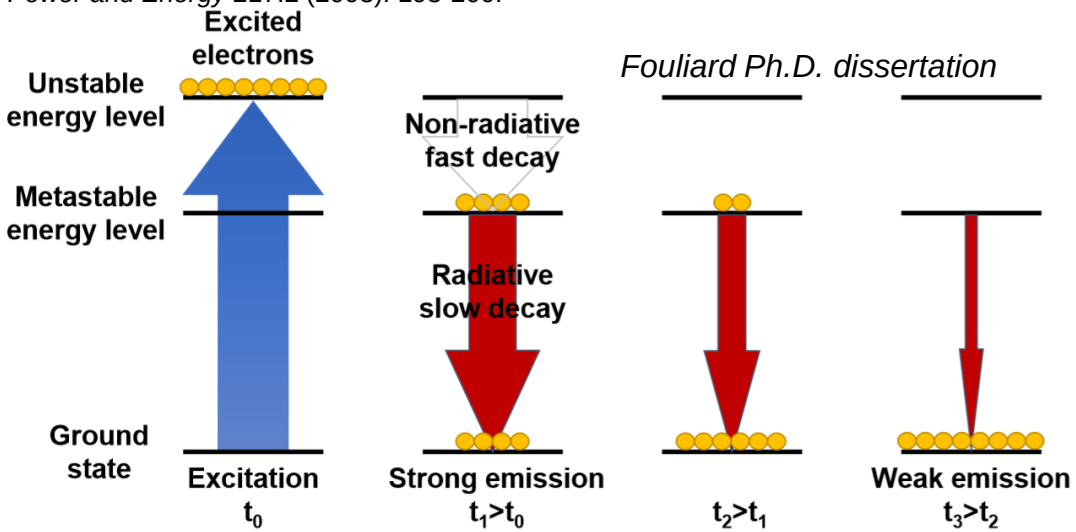

Fouliard Ph.D. dissertation

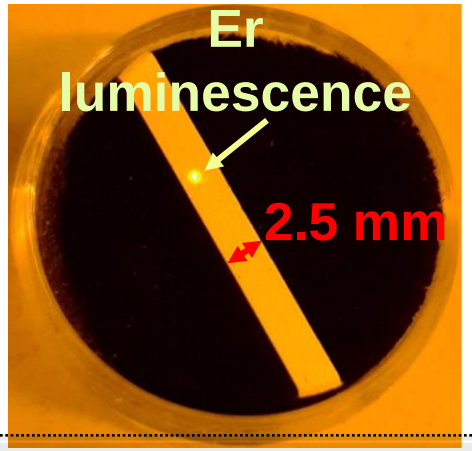

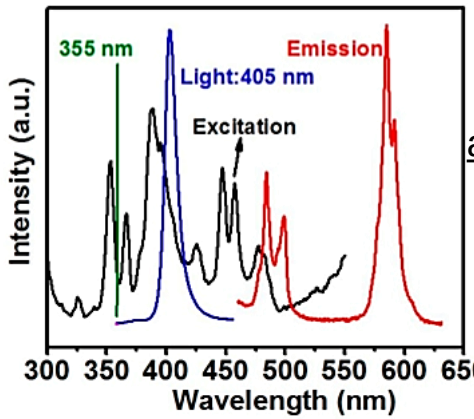

Absorption and emissio spectrum of YSZ:Dy

Peng, Di, et al. *Sensors* 16.10 (2016): 1490.

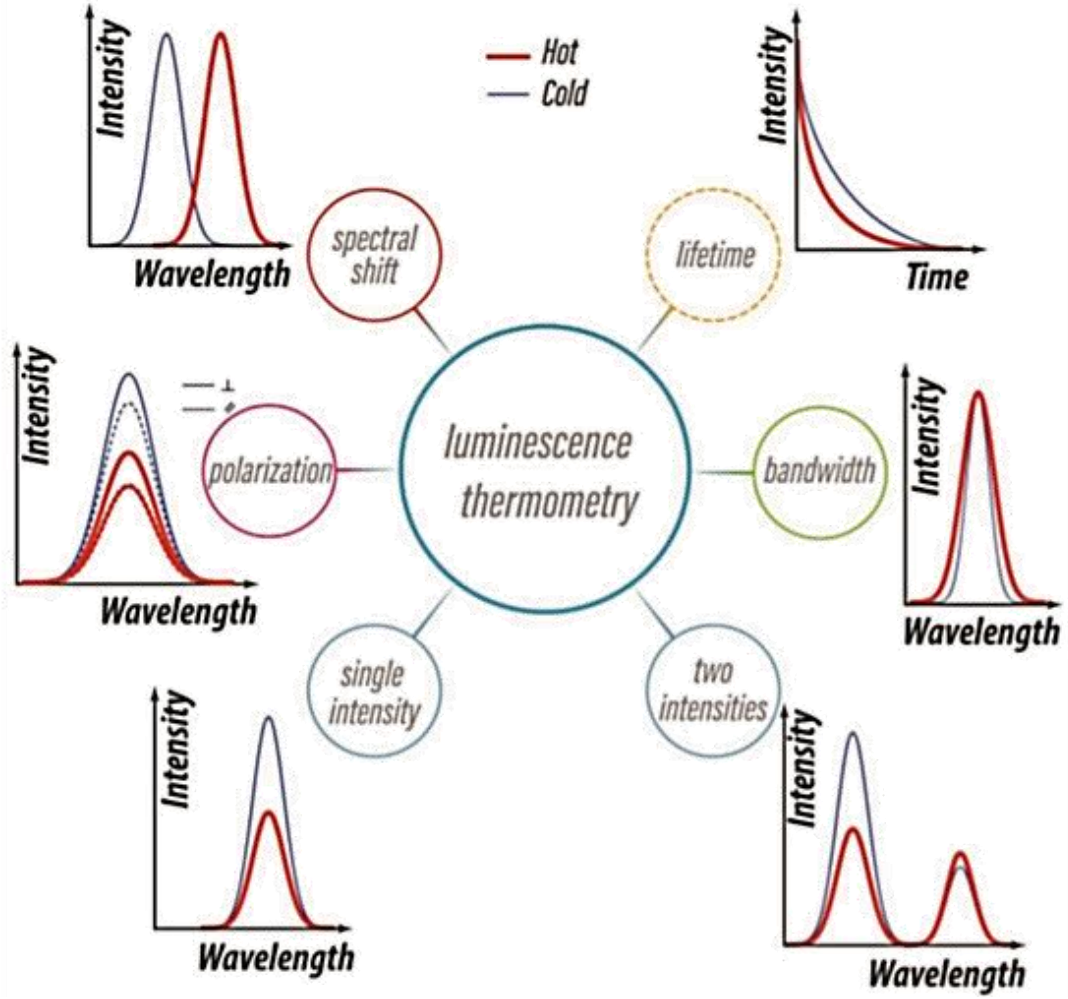

Brites, Carlos DS, Sangeetha Balabhadra, and Luís D. Carlos. "Lanthanide-based thermometers: at the cutting-edge of luminescence thermometry." *Advanced Optical Materials* 7.5 (2019): 1801239.

Instrumentation developed for synchronized luminescence decay collection

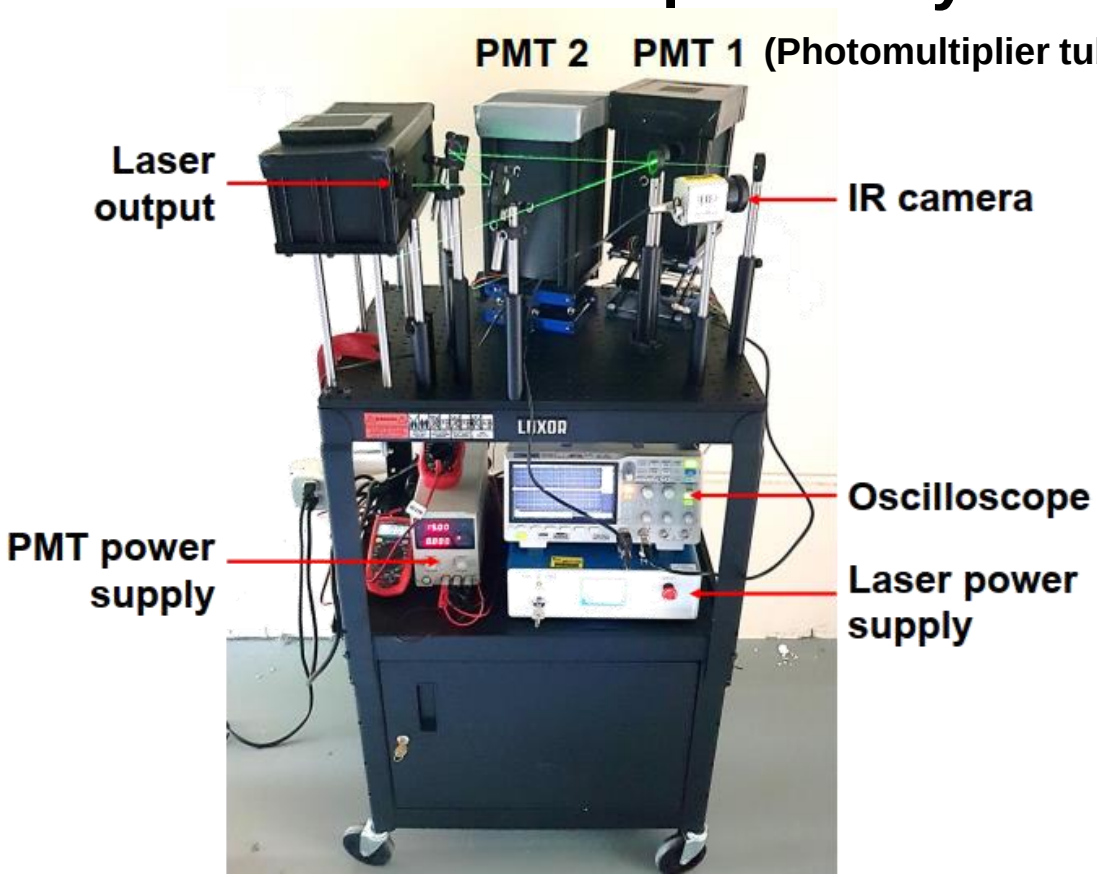

Fouliard et al., *Measurement Science & Technology*, 2020

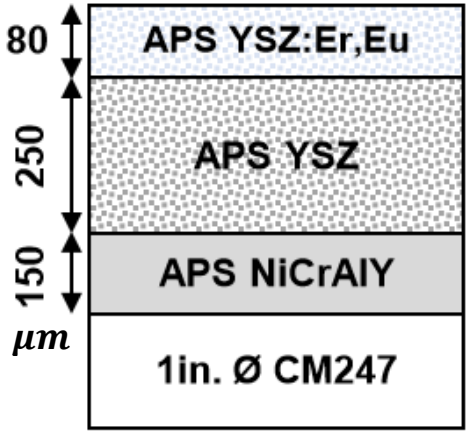

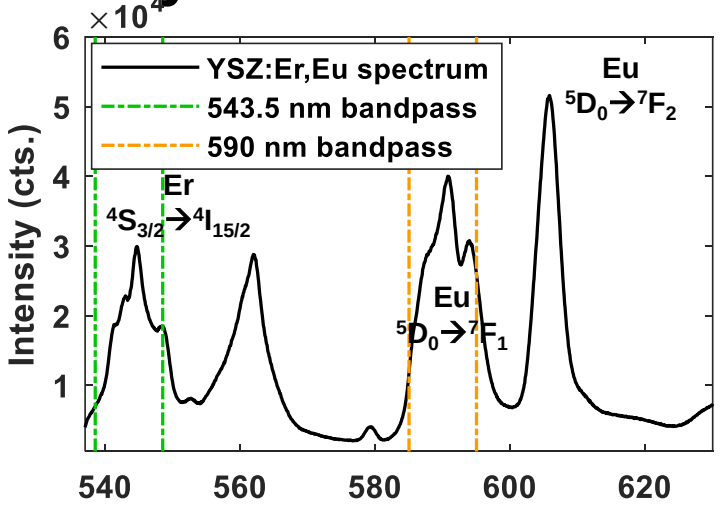

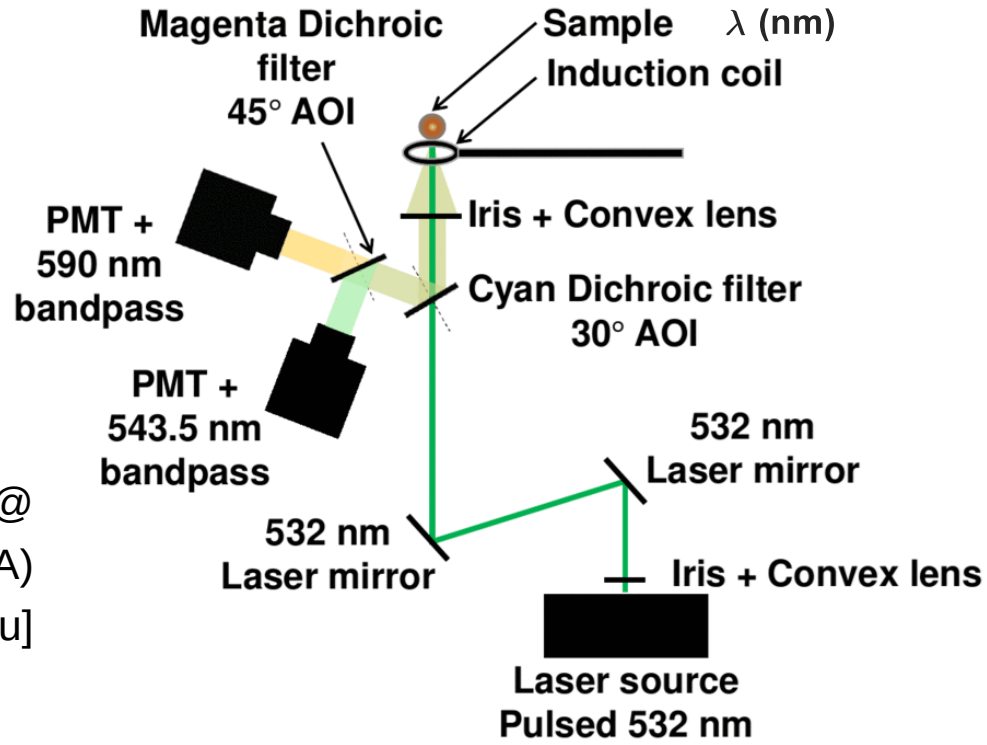

Parameters:

Nd:YAG 532 nm

0.5 mJ pulse

10 Hz

20 ns pulse duration

Sample:

Air Plasma Spray (UCF team @ FIT, Melbourne, FL, USA)

YSZ:Er,Eu [1.5% Er, 3% Eu] (Phosphor Technology, UK)

Annealed 2h @ 800˚C

Extension of temperature range vs. state-of-the-art

- Luminescence of Europium is quenched rapidly past 500°C, for high sensitivity measurements up to 850°C where reaching detector response limit.
- Temperature range extended by collecting the ratio of the normalized intensity variation Erbium/Europium.

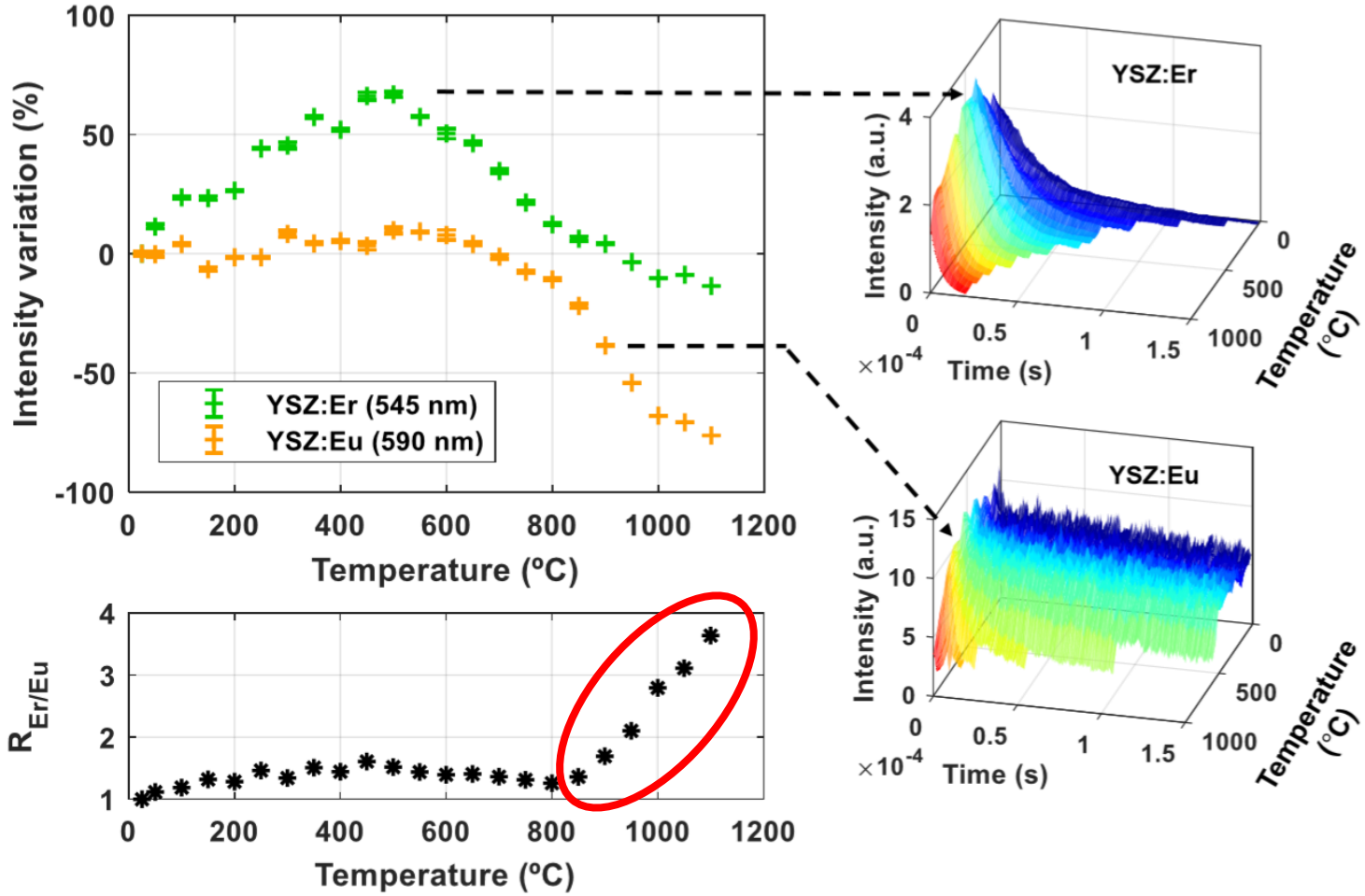

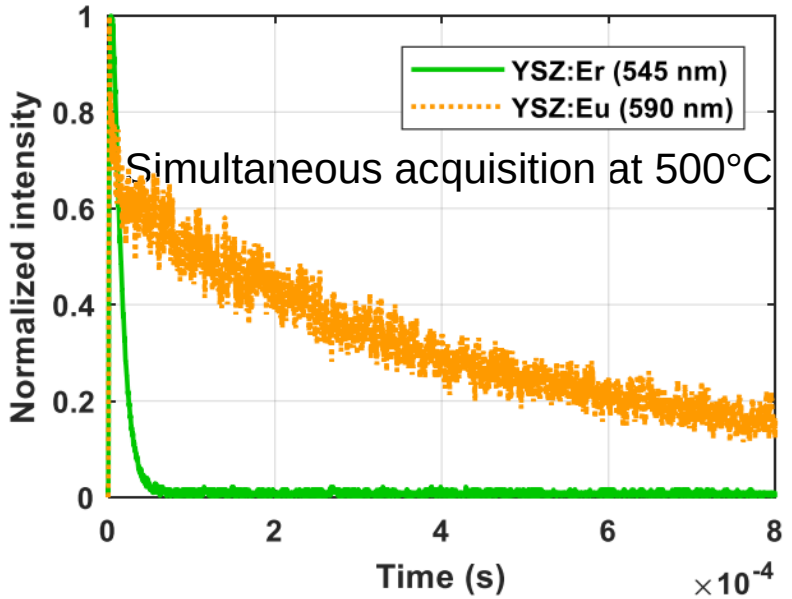

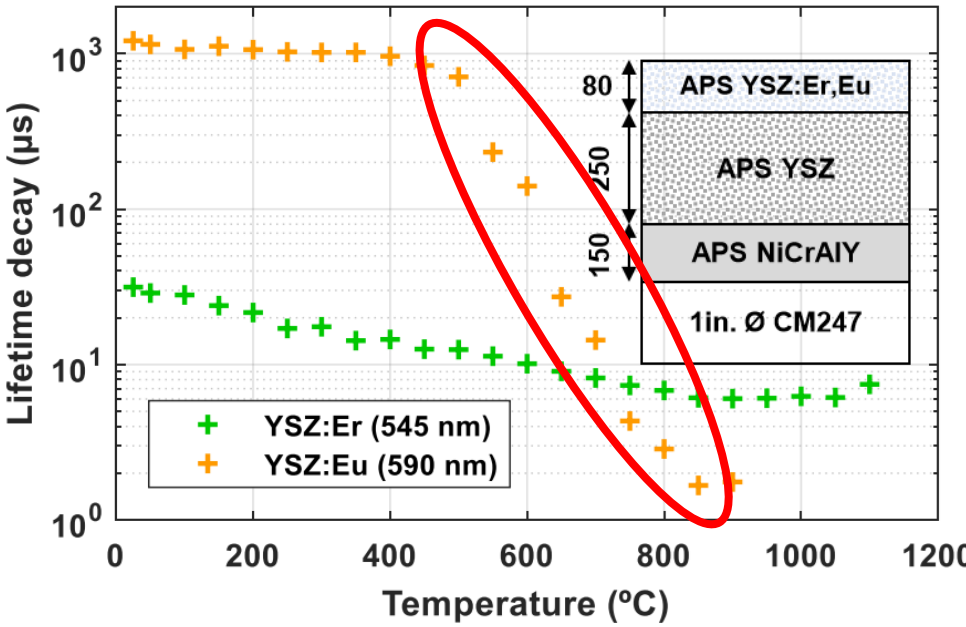

Fouliard et al., *Measurement Science & Technology*, 2020

High-speed camera testing setup for coating surface temperature measurements

A first step towards the upgrade/conversion of the setup for engine rig testing was to enable surface measurement:

→ Completed successfully with:

- High-speed camera (Photron Nova S12):
  - 250k frames/s
  - 128x128 pixel resolution
  - ISO 64,000
- Infrared camera (TIM450) – reference meas.:
  - Longwave (7.5-13 microns)
  - Emissivity set to 0.93

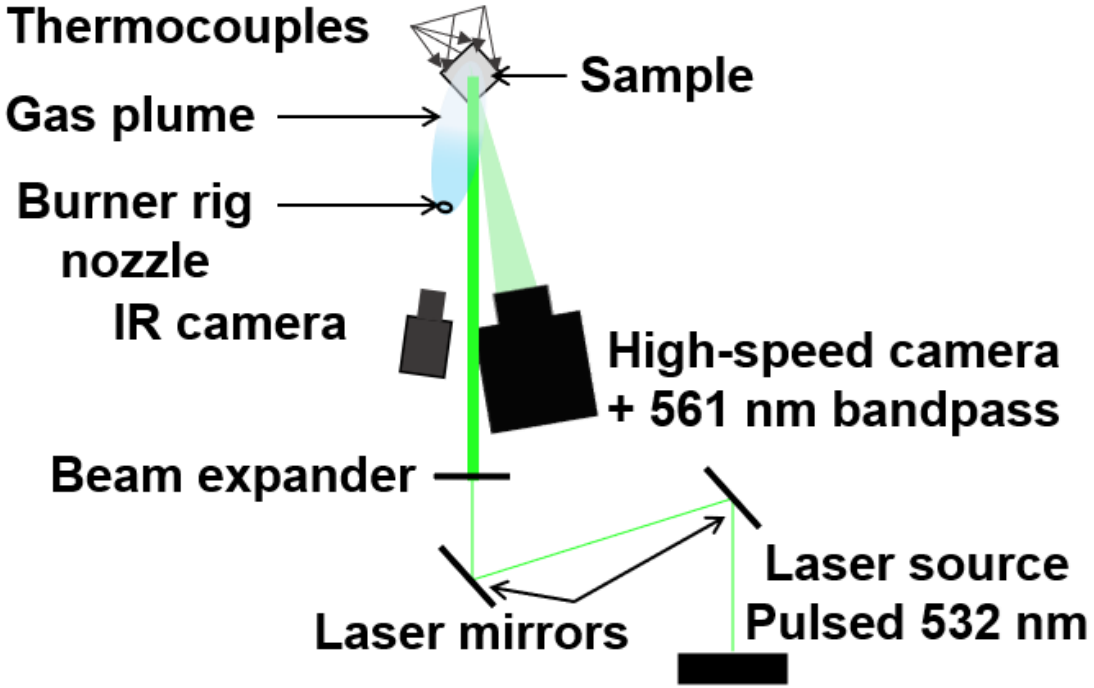

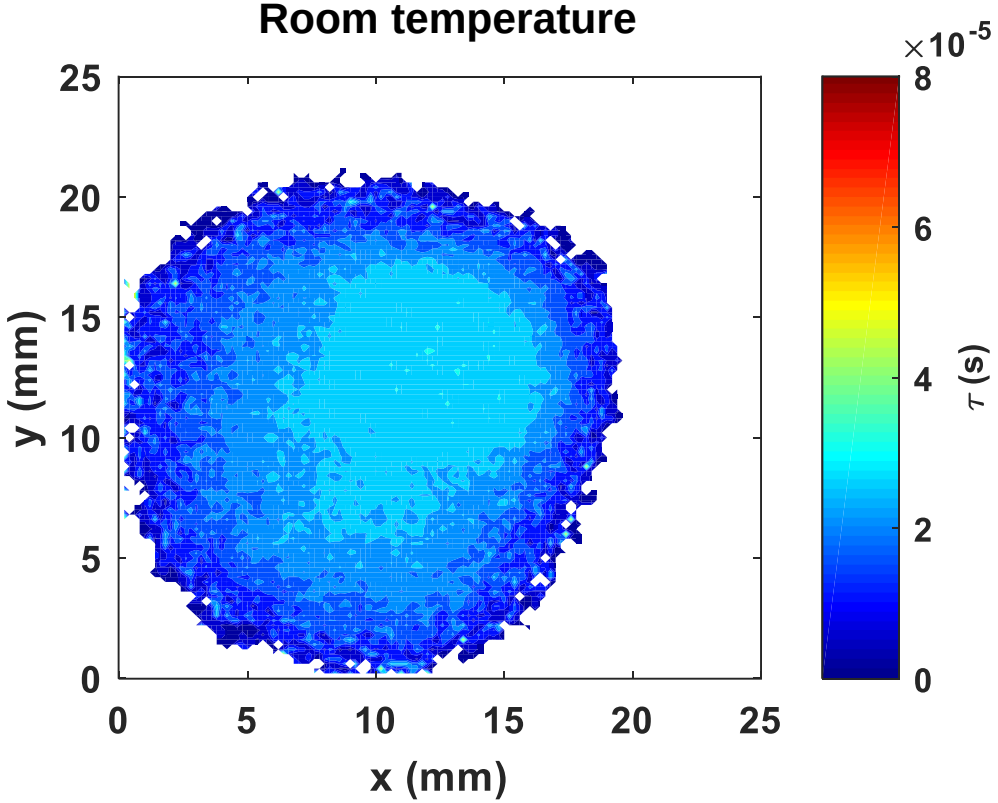

- Lifetime decay needs to be calibrated for each pixel for high temperature measurements and quantifying temperature gradients on coating surface

High-speed camera testing – heating and measurement methods:

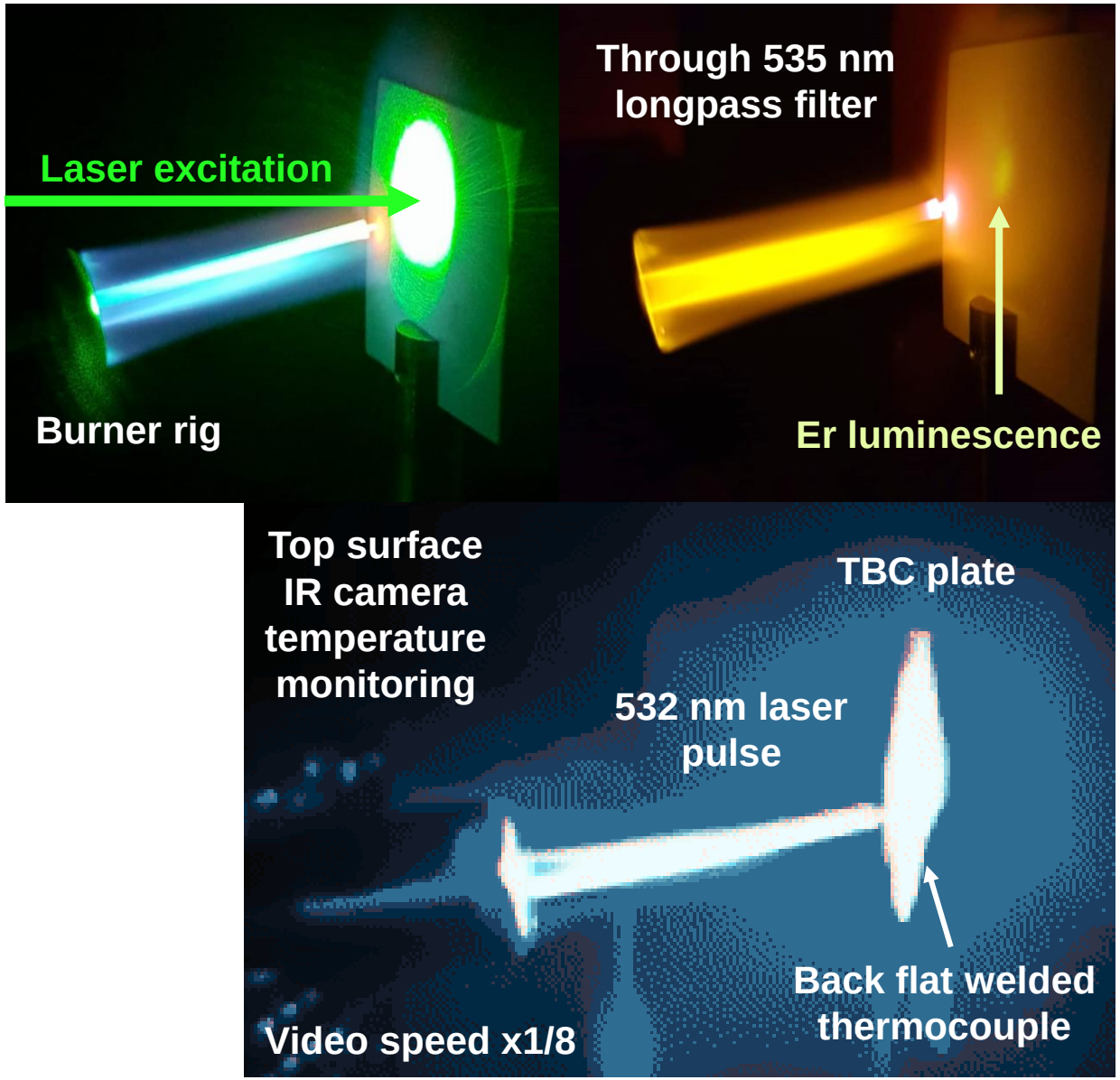

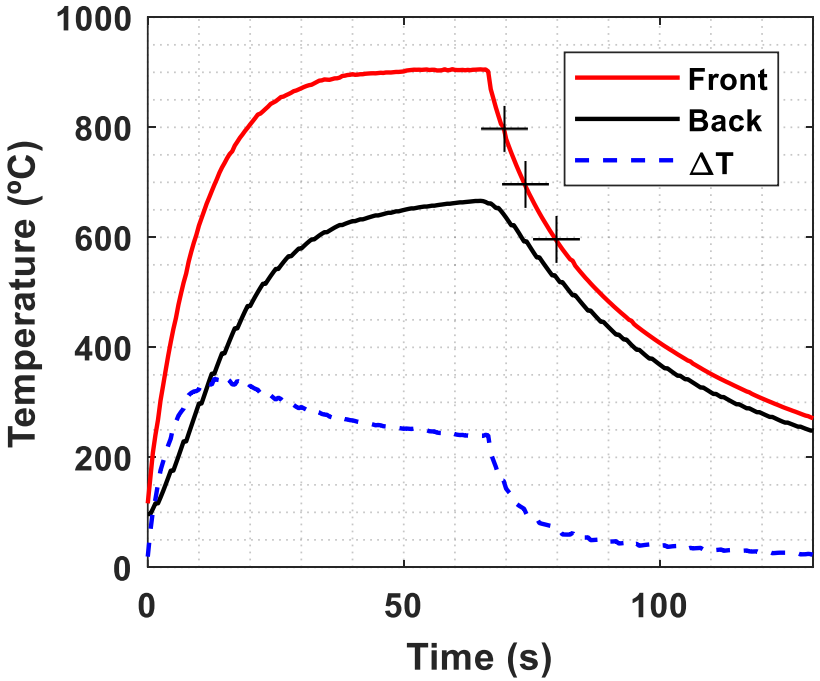

- Initial temperature measurements achieved during cooling down phase

High-speed camera testing – initial measurements:

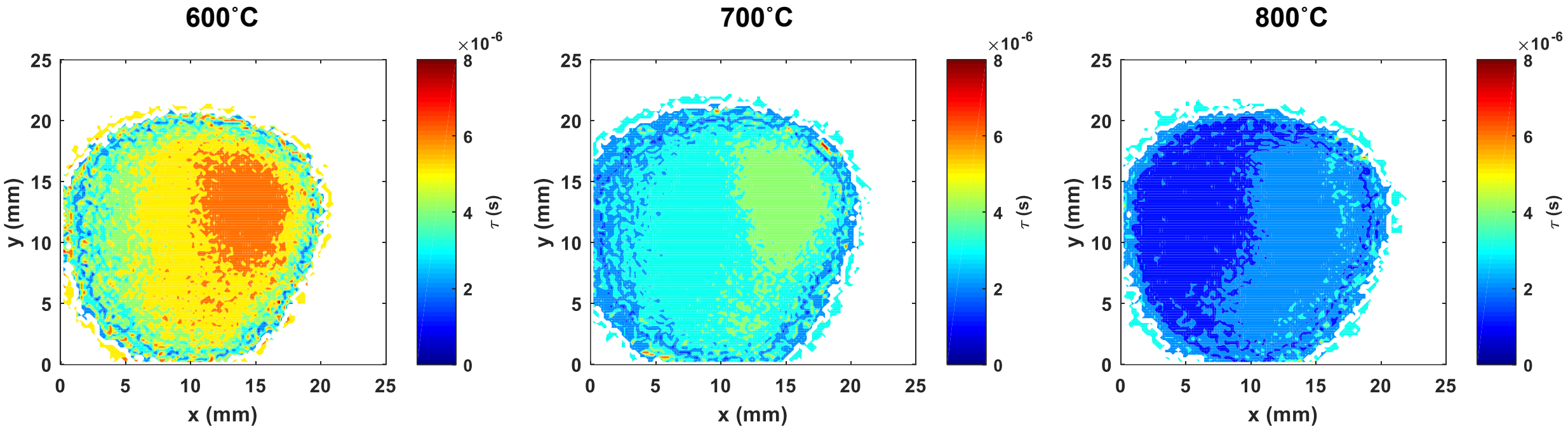

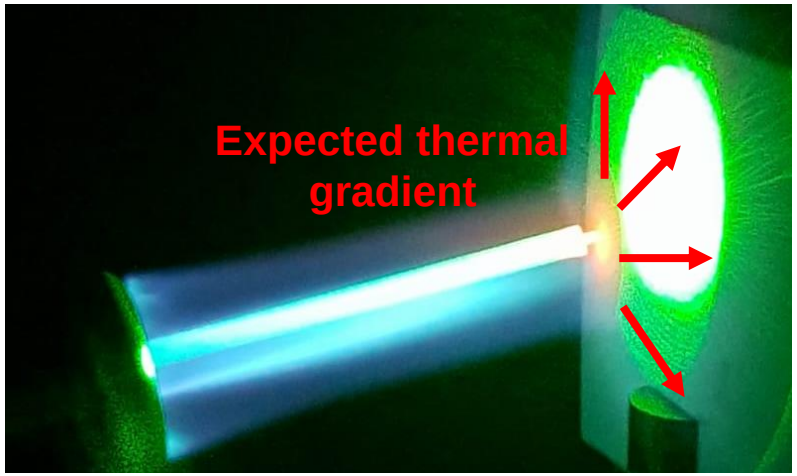

- Initial temperature measurements tend to show temperature gradient from left (hotter, faster decay) to right (colder, slower decay)
- Current work involves pixel-decay calibration

Part B: Coating damage monitoring

Part of tasks 3 & 4

Modeling delamination

Diffuse external reflectivity

$$\rho_0(n) = \frac{1}{2} + \frac{(3n+1)\cdot(n-1)}{6\cdot(n+1)^2} + \frac{n^2\cdot(n^2-1)^2}{(n^2+1)^3}\cdot\ln\left(\frac{n-1}{n+1}\right) - \frac{2n^3\cdot(n^2+2n-1)}{(n^2+1)\cdot(n^4-1)} + \frac{8n^4\cdot(n^4+1)}{(n^2+1)\cdot(n^4-1)^2}\cdot\ln(n)$$

Max diffuse internal reflectivity

$$\rho_{i,max}(n) = \left(1-\frac{1}{n^2}\right) + \frac{\rho_0(n)}{n^2}$$

Frustrated angle-averaged reflectivity

$$\overline{R}_f(d) = \frac{\int_0^{2\pi}\int_{\theta_c}^{\frac{\pi}{2}} \frac{\alpha\cdot\sinh^2(\beta\cdot d)}{1+\alpha\cdot\sinh^2(\beta\cdot d)}\cos\theta\cdot\sin\theta\, d\theta d\varphi}{\int_0^{2\pi}\int_{\theta_c}^{\frac{\pi}{2}}\cos\theta\cdot\sin\theta\, d\theta d\varphi}$$

$$\alpha_\perp = \frac{(n^2-1)^2}{4n^2\cdot\cos^2\theta\cdot(n^2\sin^2\theta-1)}$$

$$\alpha_\parallel = \alpha_\perp\cdot(\sin^2\theta\cdot(n^2+1)-1) \qquad \overline{R}_{f,unp} = \frac{\overline{R}_{f,\perp}+\overline{R}_{f,\parallel}}{2}$$

$$\beta = \frac{2\pi}{\lambda_0}\sqrt{n^2\cdot\sin^2\theta-1}$$

$$\rho_i(d) = \overline{R}_{f,unp}(d)\cdot\left(1-\frac{1}{n^2}\right) + \frac{\rho_0(n)}{n^2}$$

Q. Fouliard, R. Ghosh, S. Raghavan *Surface and Coatings Technology* (2020): 126153.

Layer	**n**	$\rho_{i,max}$
Air	**1**	84%
Top coat	2.17	39%
TGO	1.76	
Top coat - Bond coat		4%

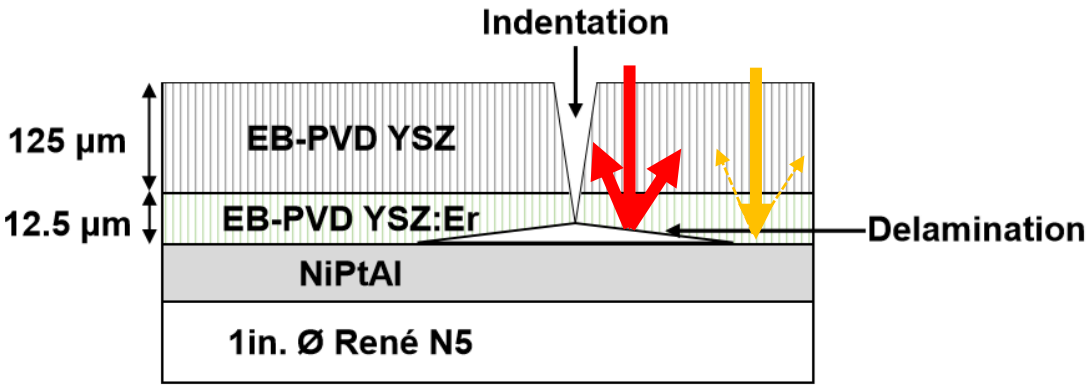

Photoluminescence results

2 sensor EB-PVD TBC configurations including an YSZ:Er layer (provided by NASA Glenn / PSU) were characterized by luminescence mapping (tracking of Er-line at 562 nm):

Sensing layer at the top

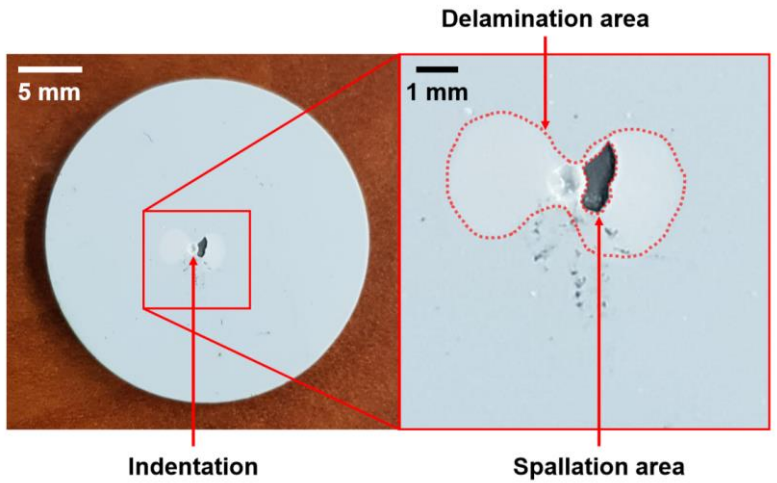

Sensing layer at the bottom

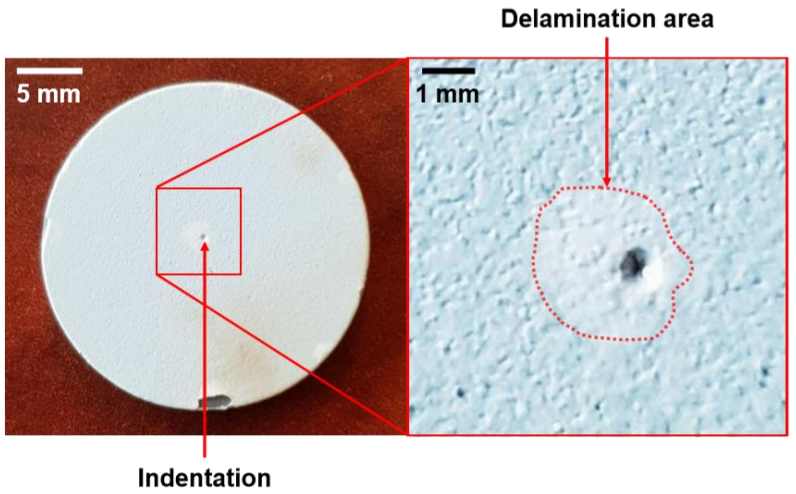

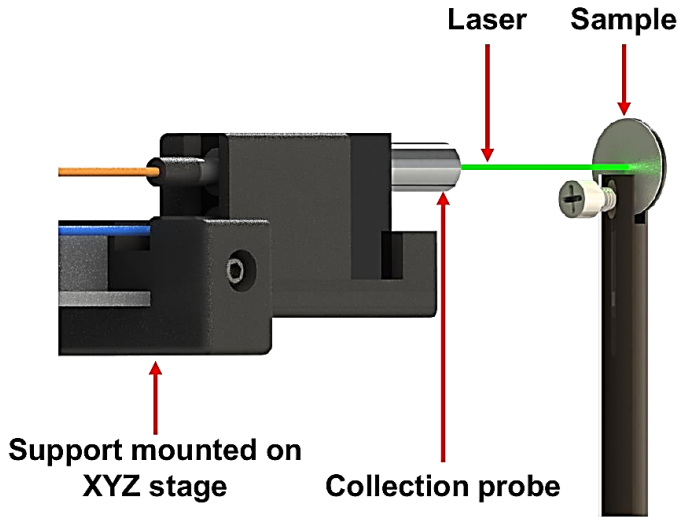

Q. Fouliard, et al. Surface and Coatings Technology (2020)

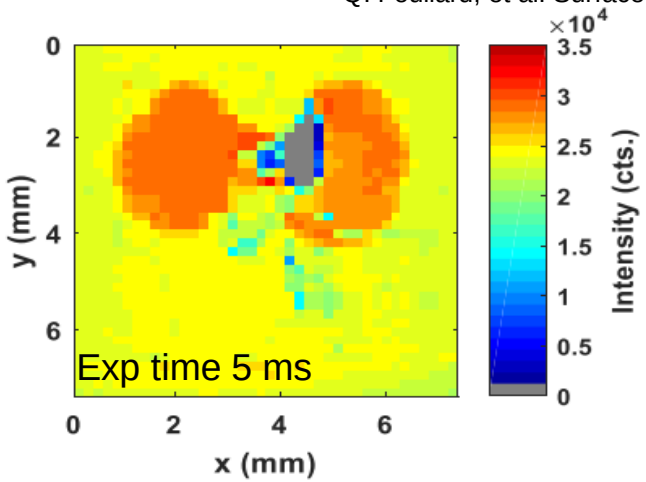

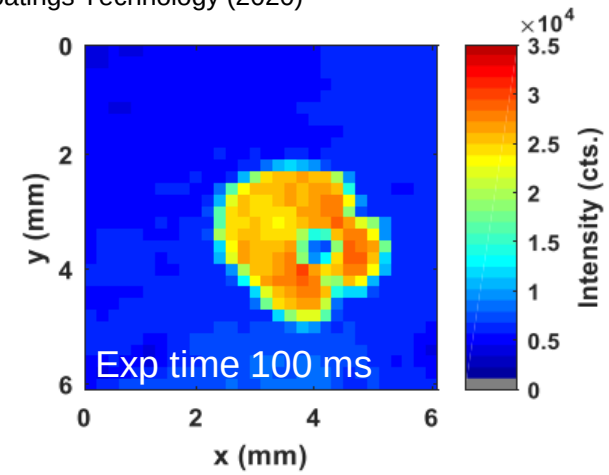

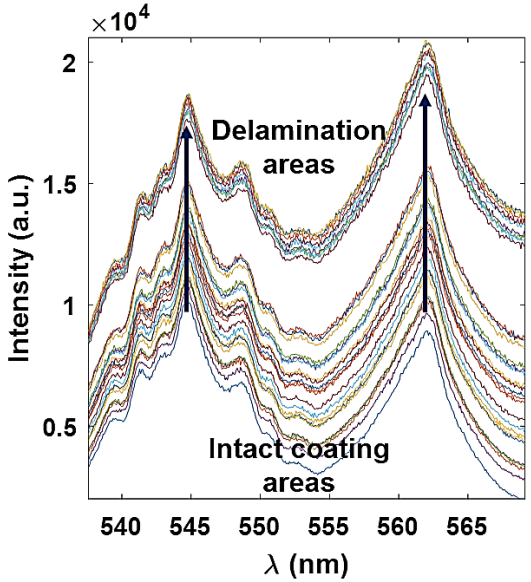

15 mW,
532 nm excitation
Focal length:
7.5 mm
Depth of field:
2.2 mm
Numerical aperture:
0.27
Spot size: 200 µm

Modeling luminescence intensity based on a 2x2 flux Kubelka-Munk model

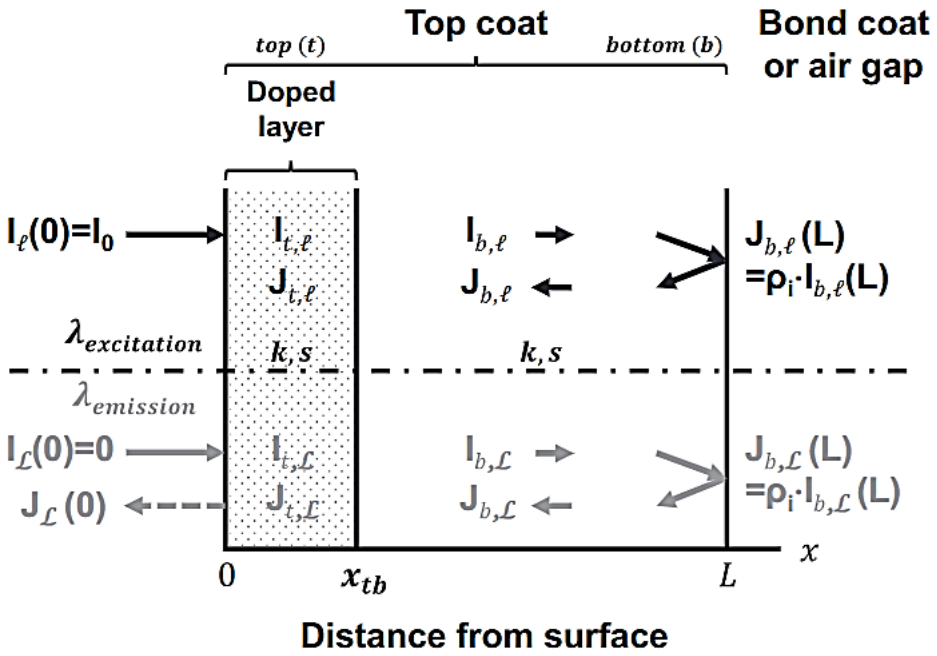

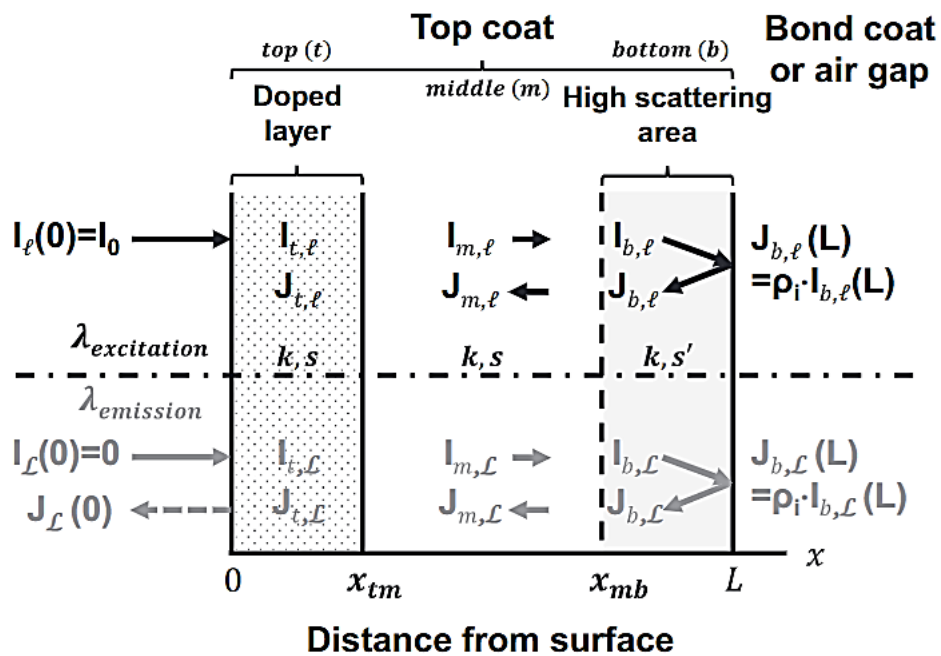

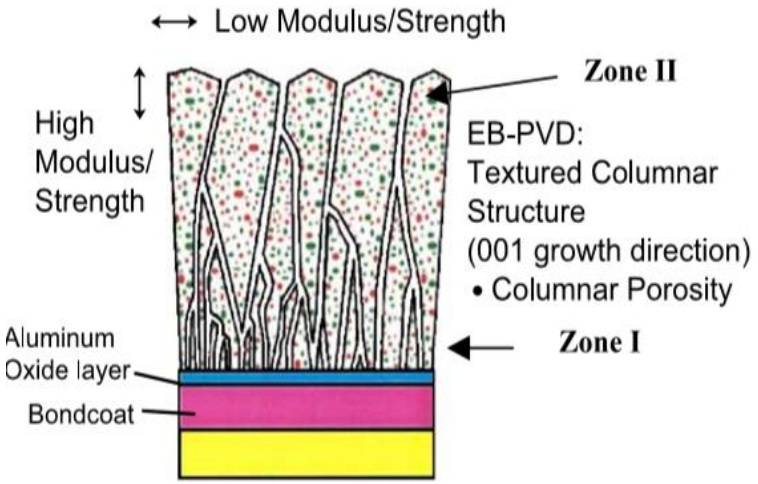

Wolfe, Douglas E., et al *Surface and Coatings Technology* 190.1 (2005): 132-149.

$$Y_\lambda(x) = [I_{t,\lambda}(x)\ J_{t,\lambda}(x)\ I_{m,\lambda}(x)\ J_{m,\lambda}(x)\ I_{b,\lambda}(x)\ J_{b,\lambda}(x)]^T$$

$$A_{z,\lambda} = \begin{pmatrix} -(K_{z,\lambda} + S_{z,\lambda}) & S_{z,\lambda} \\ -S_{z,\lambda} & K_{z,\lambda} + S_{z,\lambda} \end{pmatrix} \qquad Q_z = \frac{1}{2}\begin{pmatrix} q_z K_{z,\ell} & q_z K_{z,\ell} \\ -q_z K_{z,\ell} & -q_z K_{z,\ell} \end{pmatrix}$$

$$\frac{dY_\ell(x)}{dx} = \begin{pmatrix} A_{t,\ell} & 0 & 0 \\ 0 & A_{m,\ell} & 0 \\ 0 & 0 & A_{b,\ell} \end{pmatrix} \cdot Y_\ell(x)$$

$$\frac{dY_{\mathcal{L}}(x)}{dx} = \begin{pmatrix} A_{t,\mathcal{L}} & 0 & 0 \\ 0 & A_{m,\mathcal{L}} & 0 \\ 0 & 0 & A_{b,\mathcal{L}} \end{pmatrix} \cdot Y_{\mathcal{L}}(x) + \begin{pmatrix} Q_t & 0 & 0 \\ 0 & Q_m & 0 \\ 0 & 0 & Q_b \end{pmatrix} \cdot Y_\ell(x)$$

Delamination monitoring: Comparison experiment vs. model

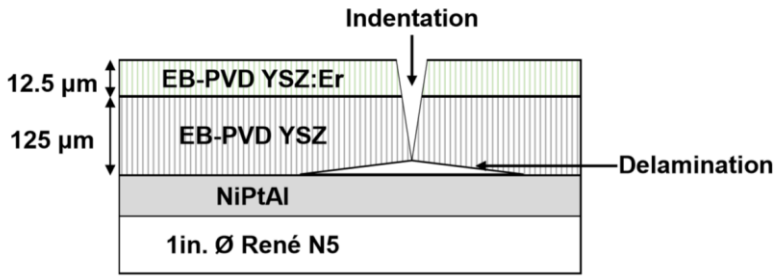

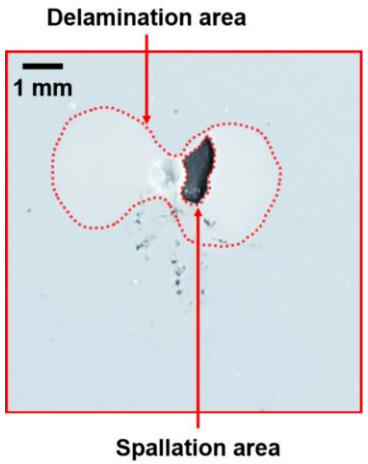

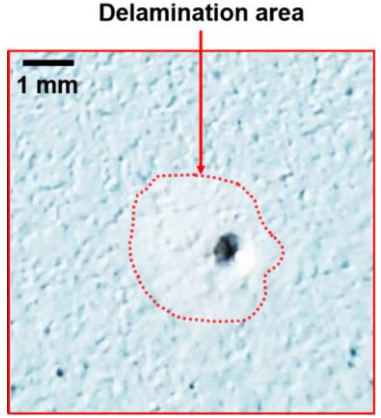

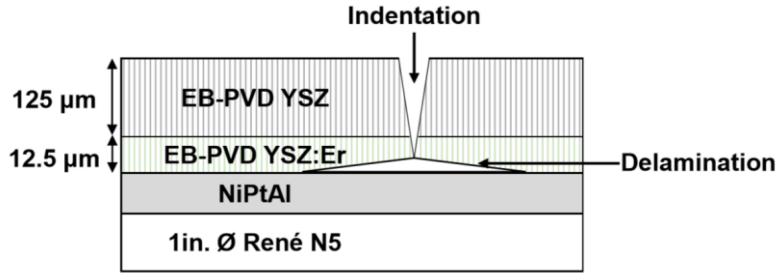

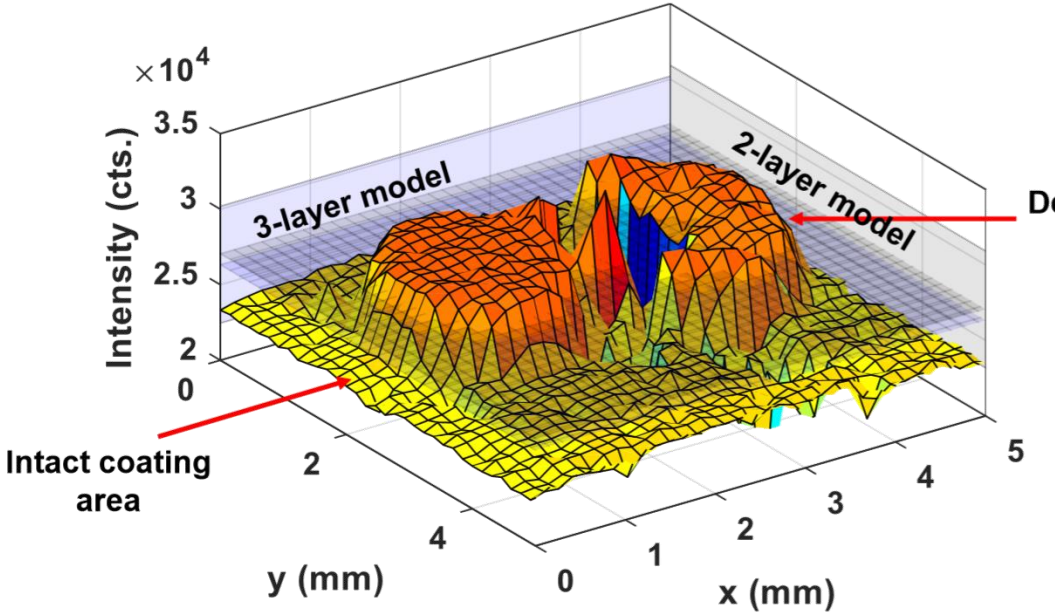

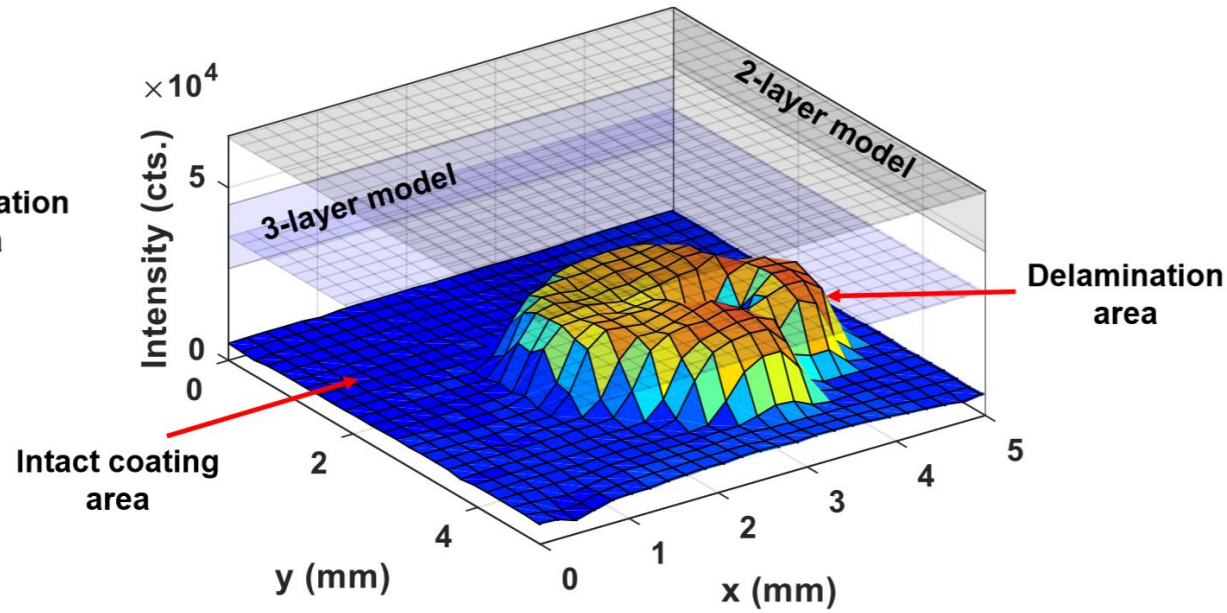

Q. Fouliard, R. Ghosh, S. Raghavan *Surface and Coatings Technology* (2020): 126153.

Novel approach for delamination sensing using λ-dependent optical properties

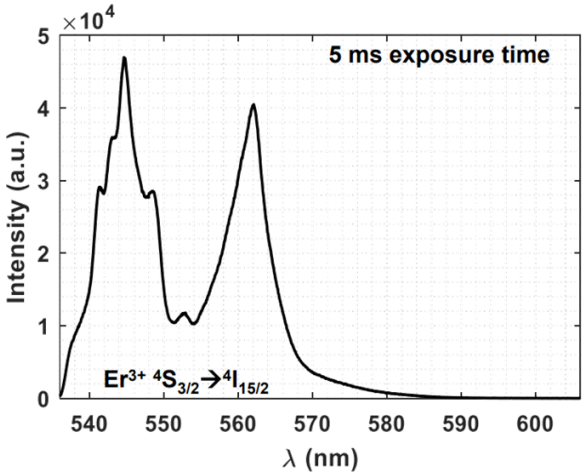

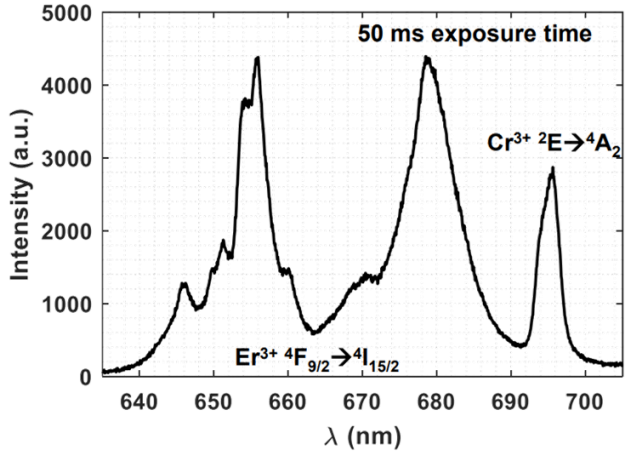

Luminescence contrast	λ	Sample A	Sample B
Kubelka-Munk model	545 nm	1.09 ± 0.01	6.05 ± 0.62
	562 nm	1.10 ± 0.01	6.22 ± 0.63
	655 nm	1.12 ± 0.01	6.69 ± 0.62
	680 nm	1.13 ± 0.01	6.74 ± 0.61
Experimental measurement	545 nm	1.18 ± 0.02	4.20 ± 0.24
	562 nm	1.20 ± 0.02	5.31 ± 0.29
	655 nm	1.22 ± 0.03	5.95 ± 0.53
	680 nm	1.22 ± 0.06	6.63 ± 1.01

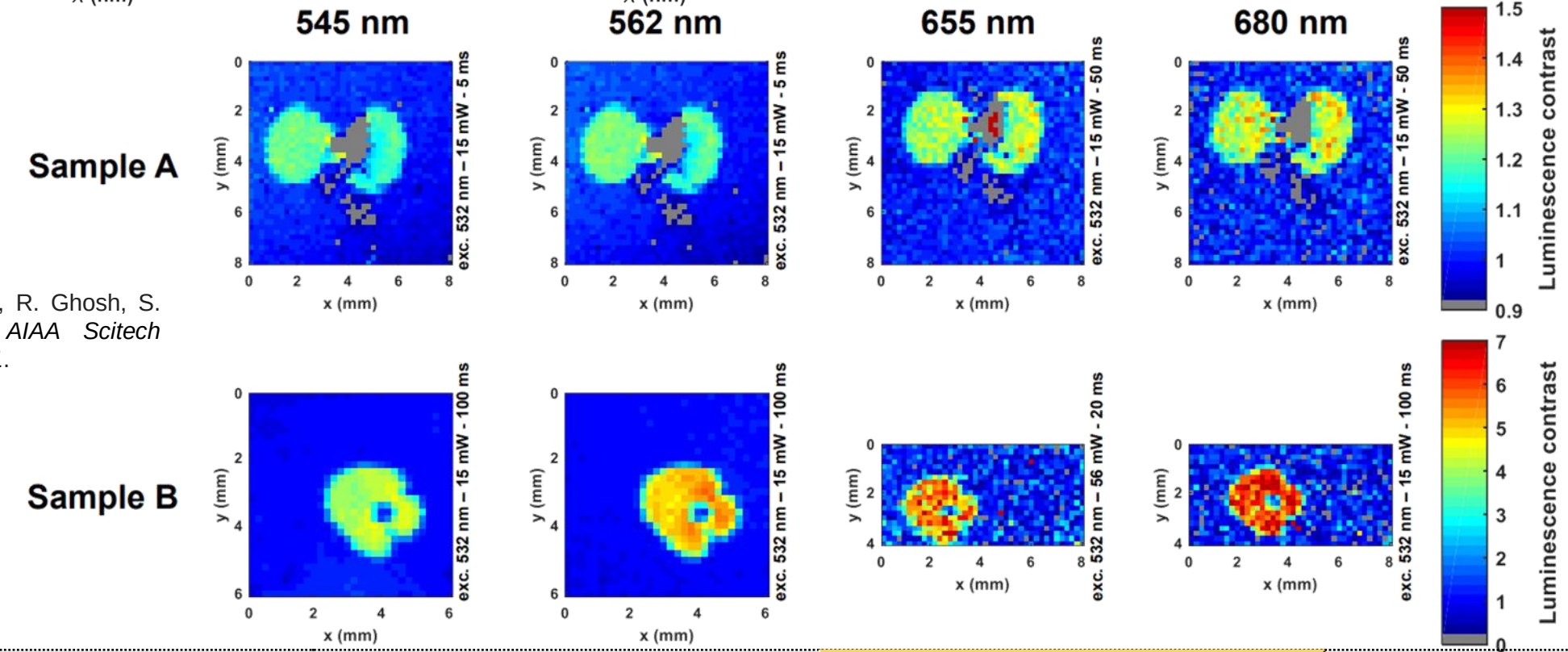

Q. Fouliard, R. Ghosh, S. Raghavan *AIAA Scitech Forum 2021*.

Conclusions & Perspectives

Conclusions

- Precise determination of temperatures in TBCs can result in large benefits in terms of fuel savings, reduction of emission, as well as better monitoring of TBC lifetime
- Enabled the extension of the range of measurable temperatures using phosphor thermometry with higher sensitivity by capturing simultaneously luminescence decays and intensities using a co-doped YSZ:Er,Eu sensor TBC.
- Developed surface temperature measurement capabilities using a high-speed camera setup.
- Currently extending the instrument to engine rig setup for in-situ temperature measurements.
- Enabled accurate determination of delamination in coatings through a novel modeling approach, validated with experiments.

Future work

Ongoing work with collaborators that was initiated with this project:

- Additional synchrotron experiments for rare-earth doped TBC strain measurements (collaboration: GE Research, Argonne National Lab).
- Model adaptation and experimentation using high-emissivity paints for improved temperature measurements on painted TBCs (collaborator: GE Aviation).

Task 6:

- Continuation of high-speed camera testing and analysis work.
- Adaptation of the instrumentation to operate on an engine rig (Tasks 1-5 successfully demonstrated lab-scale functionality as planned – the existing built-up will now be adapted to rapidly increase its technology readiness level), starting with the exhaust section of UCF (Dr. Ahmed) ramjet engine and going towards more challenging engine sections like high-pressure turbines or RDE walls.

Patents

- Quentin Fouliard, Ranajay Ghosh, Seetha Raghavan, “System and Method to Reveal Temperature Gradients Across Thermal Barrier Coatings Using Phosphor Thermometry”, U.S. Patent Serial No. 17/034,156, 09/2020
- Quentin Fouliard, Ranajay Ghosh, Seetha Raghavan, “Phosphor Thermometry System for Synchronized Luminescence Lifetime Decay Measurements”, U.S.Patent Serial No. 62/944,390,12/2019
- Quentin Fouliard, Ranajay Ghosh, Seetha Raghavan, “Rare-Earth Doped Thermal Barrier Coating Bond Coat for Thermally Grown Oxide Luminescence Sensing”, U.S.Patent Serial No. 62/940,963,11/2019

Publications

- Quentin Fouliard, Johnathan Hernandez, Hossein Ebrahimi, Khanh Vo, Frank Accornero, Mary McCay, Jun-Sang Park, Jonathan Almer, Ranajay Ghosh, Seetha Raghavan ”Synchrotron X-Ray Diffraction To Quantify In-Situ Strain On Rare-Earth Doped Yttria-Stabilized Zirconia Thermal Barrier Coatings”, ASME Turbo Expo 2021: Turbomachinery Technical Conference & Exposition. American Society of Mechanical Engineers, 2021. (Accepted)
- Quentin Fouliard, Ranajay Ghosh, and Seetha Raghavan. "Delamination of Electron-Beam Physical-Vapor Deposition Thermal Barrier Coatings using Luminescent Layers.“ 2021 AIAA SciTech Forum
- Quentin Fouliard, Ranajay Ghosh, Seetha Raghavan, “Quantifying thermal barrier coating delamination through luminescence modeling”, Surface and Coatings Technology, 126153, 2020
- Quentin Fouliard, Johnathan Hernandez, Bauke Heeg, Ranajay Ghosh, Seetha Raghavan, “Phosphor Thermometry Instrumentation for Synchronized Acquisition of Luminescence Lifetime Decay on Thermal Barrier Coatings”, Measurement Science and Technology 31(5), 054007, 2020
- Quentin Fouliard, Sandip Haldar, Ranajay Ghosh, and Seetha Raghavan. “Modeling luminescence behavior for phosphor thermometry applied to doped thermal barrier coating configurations.” Applied Optics 58(13), D68-D75, 2019
- Quentin Fouliard, Ranajay Ghosh, Seetha Raghavan, “Doped 8% Yttria-Stabilized Zirconia for Temperature Measurements on Thermal Barrier Coatings using Phosphor Thermometry”, 2020 AIAA SciTech Forum, Orlando, FL, January 6-10, 2020
- Sandip Haldar, Peter Warren, Quentin Fouliard, […], Ranajay Ghosh, Seetha Raghavan, “Synchrotron XRD measurements of Thermal Barrier Coating Configurations With Rare Earth Elements For Phosphor Thermometry”, ASME Turbo Expo 2019: Turbine Technical Conference and Exposition GT2019, Phoenix, AZ, June 17-21, 2019
- Quentin Fouliard, Sanjida A. Jahan, Lin Rossmann, Peter Warren, Ranajay Ghosh, Seetha Raghavan, “Configurations for Temperature Sensing of Thermal Barrier Coatings,” 1st International Conference on Phosphor Thermometry (ICPT 2018), Glasgow, UK, July 25-27, 2018

Acknowledgments

Collaborators

Lumium — Bauke Heeg

Florida Institute of Technology — Mary McCay, Frank Accornero, David Moreno

Argonne National Laboratory — Jonathan Almer, Jun Sang-Park

GE — Ed Hoffmann, Joshua Salisbury

NASA — Jeffrey Eldridge

SIEMENS — Dr. Ramesh Subramanian

This material is based upon work supported by the U.S. Department of Energy, National Energy Technology Laboratory, University Turbine Systems Research (UTSR) under Award Number: DE-FE0031282.

THANK YOU FOR YOUR ATTENTION

CONTACT EMAILS AND WEBSITE

seetha.raghavan@ucf.edu

quentin@knights.ucf.edu

https://aerostructures.cecs.ucf.edu/

ANNEX

Phosphor Thermometry – intensity ratio method

- Thermal quenching and growing thermal radiation limits luminescence detection at high temperature.
- Thermal filling of the excited states

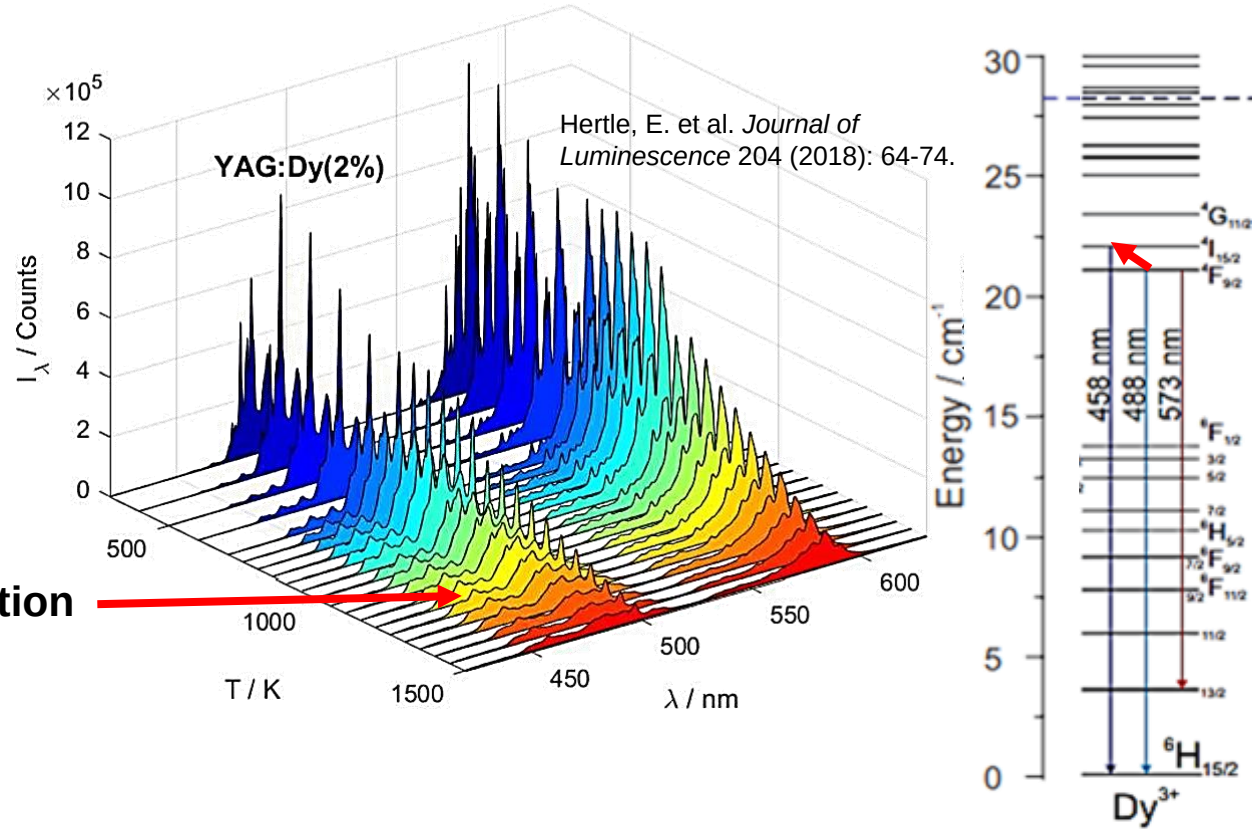

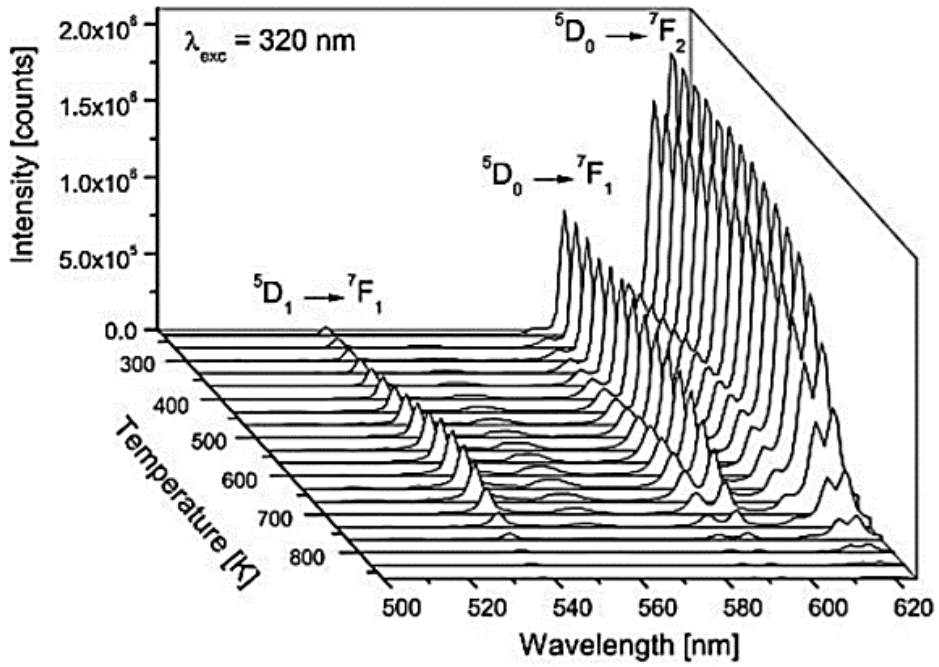

Fig. 2. Typical emission spectra of $GdVO_4$:6 mol.%Eu^{3+} sample over a temperature range of 298–823 K.

Nikolić, Marko G., Dragana J. Jovanović, and Miroslav D. Dramićanin. "Temperature dependence of emission and lifetime in Eu 3+-and Dy 3+-doped GdVO 4." *Applied optics* 52.8 (2013): 1716-1724.

Background - Phosphor Thermometry – luminescence decay method

- The time dependent intensity is measured following the excitation pulse to determine the temperature dependent decay time $\tau(T)$.

(a) *Fouliard Ph.D dissertation*

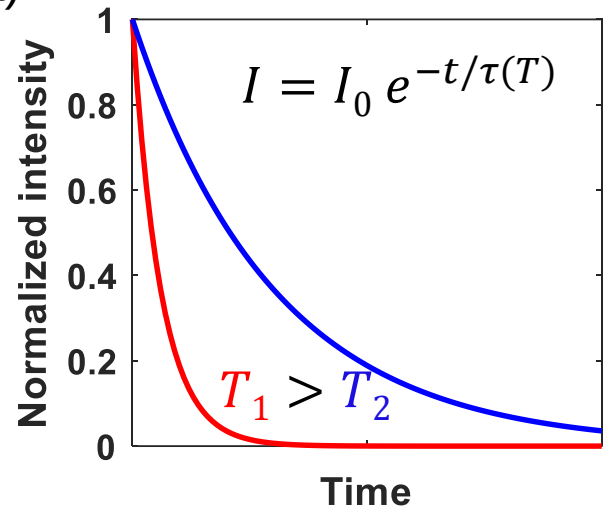

(b)

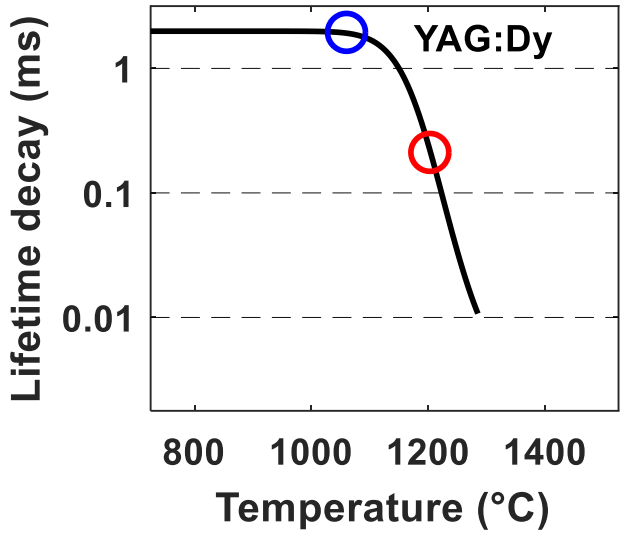

Schematic of (a) Normalized intensity vs. time for temperature T_1 and T_2, (b) correlating decay time with temperature

Luminescence lifetime decay:

$$\tau = \frac{1}{W_r + W_{nr}}$$

τ: lifetime decay,
$W_{r/nr}$: radiative and non-radiative deexcitation rates.

- Thermal quenching accelerates decay due to higher probability of vibrational deexcitation. Knappe, C. *PhD dissertation Lund University* (2013)

Absolute sensitivity:

$$S_a = \left| \frac{dQ}{dT} \right|$$

Q: sensor variable (τ or R),
T: temperature

- Higher sensitivity of the decay method in comparison with the intensity ratio method but often limited to a reduced temperature range. Heeg, et al. *AIP Conference Proceedings, Vol. 1552*, (2013)

Project extension (task 6): Instrument adaptation to engine rig

- Instrument optimization for Er and Eu luminescence sensing
- Improved filtering of gas radiation
- Multi-mode fiber collimator with high-damage threshold (0.5 mJ/pulse ≈20 ns)

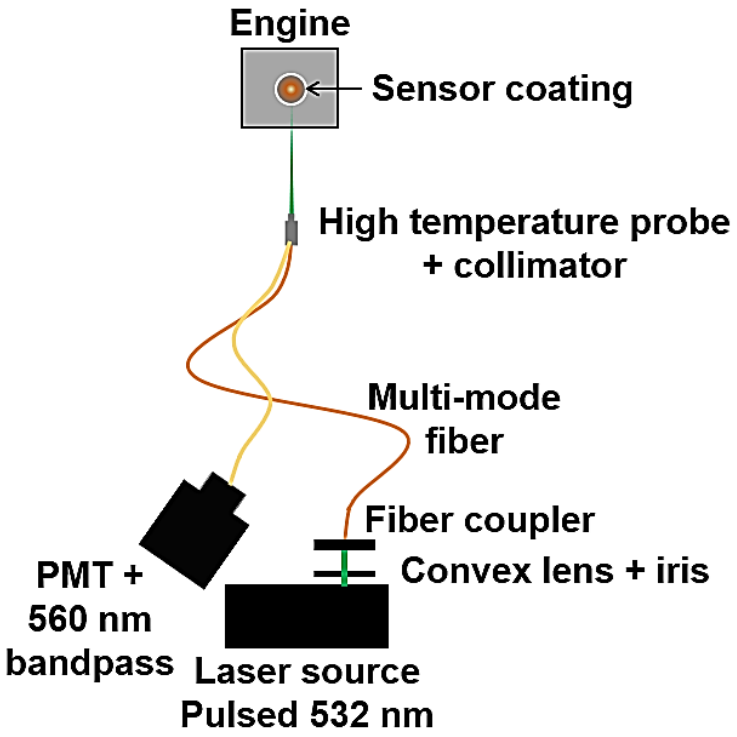

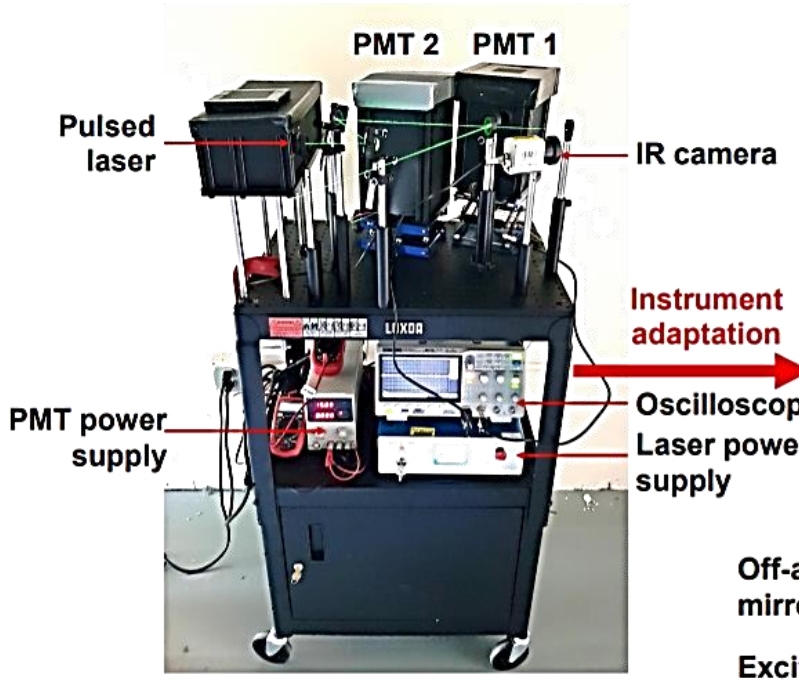

Instrument adaptation

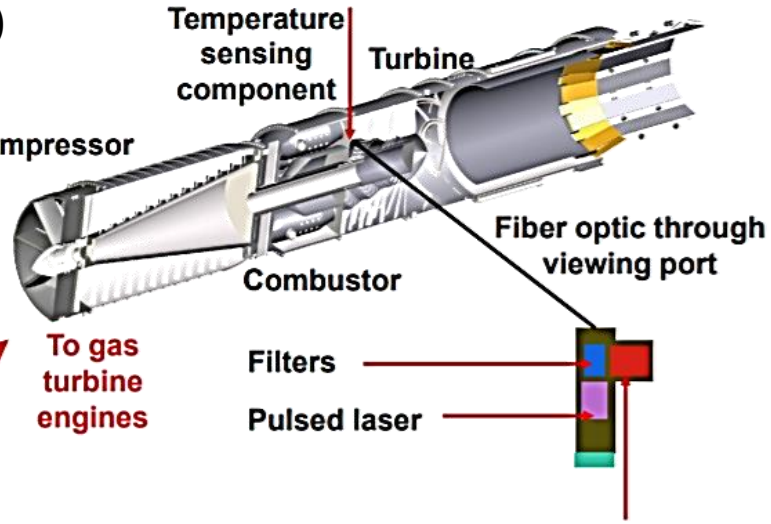

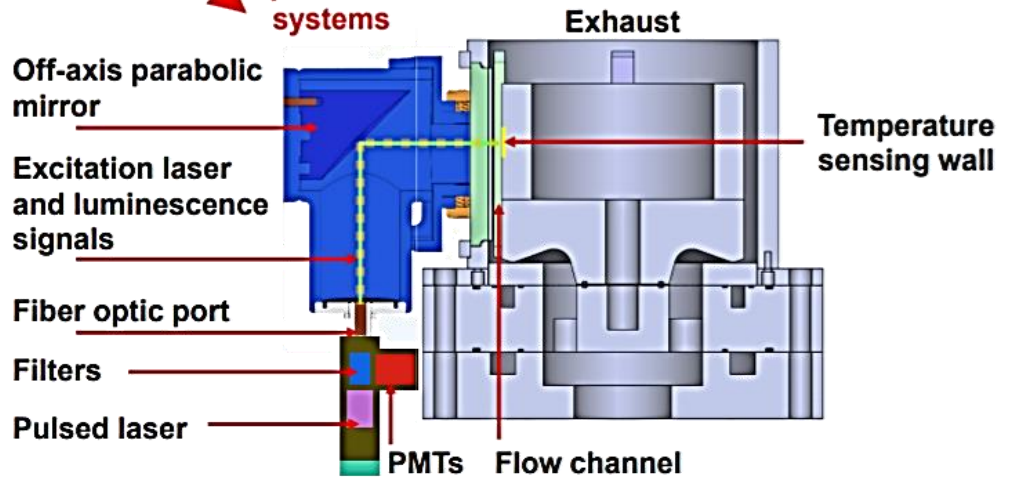

Project extension: Instrument adaptation to engine rig (initial test)

UCF Ramjet exhaust wall in-situ measurement

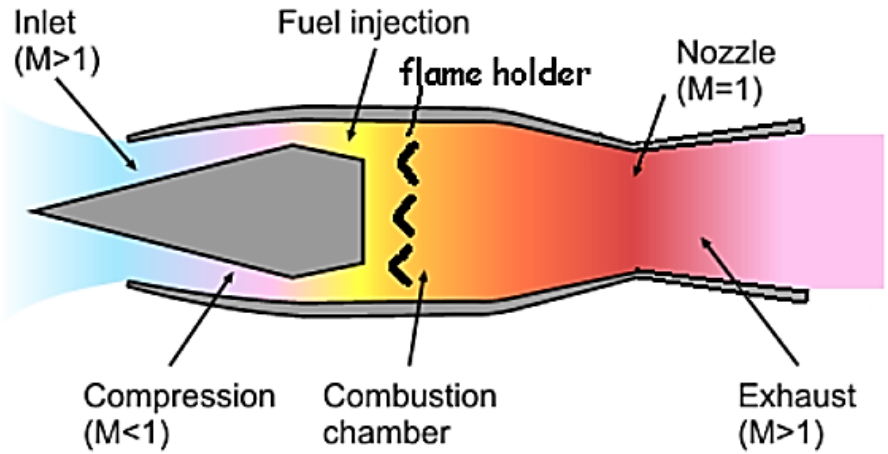

Hossain, Mohammad A., et al. *ASME International Mechanical Engineering Congress and Exposition*. Vol. 46421. ASME, 2014.

2x2” sensor plate placed at top

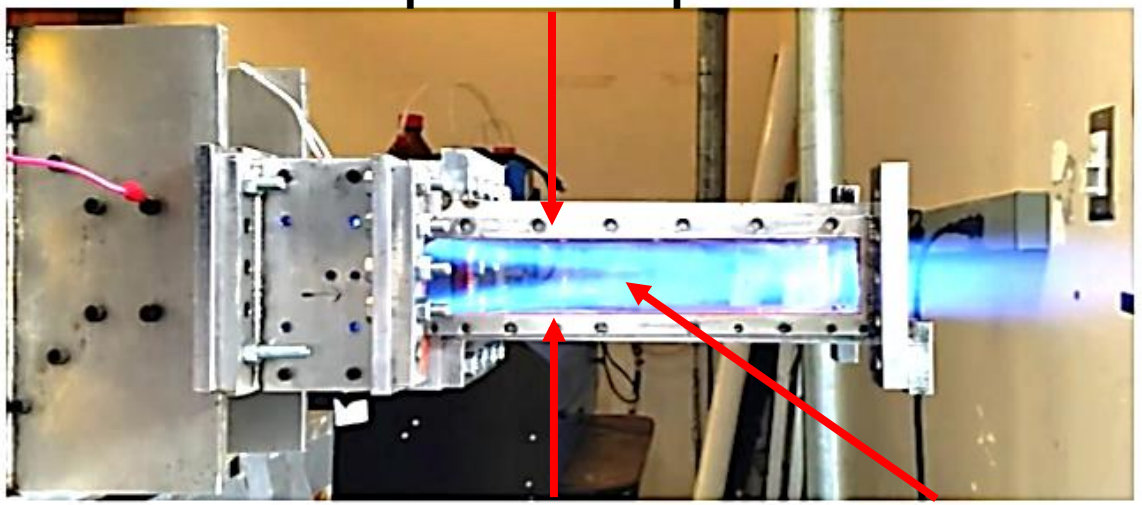

Viewing port from below for phosphor thermometry

Lateral viewing port for IR meas.

Sample configurations

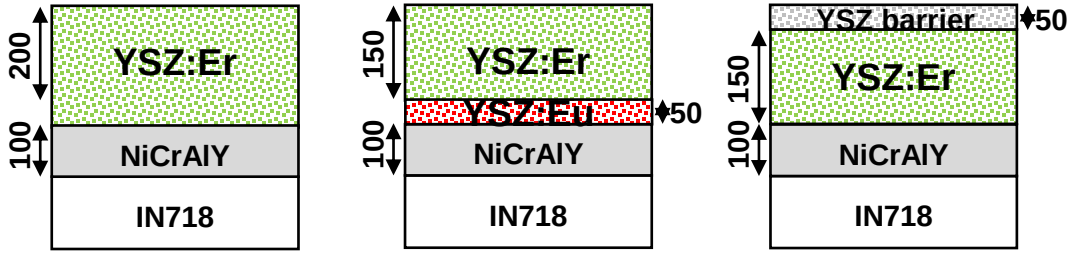

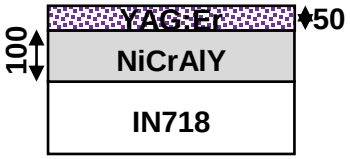

- Er has strong luminescence and close to ideal single-exponential decay
- Eu is compatible for simultaneous sensing with Er
- Higher temperatures can be measured either through non-luminescent thermal barrier or using a garnet host YAG:Er

Synchrotron XRD measurements at Argonne National Laboratory

- Strain drives cracking / delamination / spallation and is closely related to strain at the interface top coat / bond coat Schlichting, KW., et al. *Materials Science and Engineering: A* 342.1-2 (2003): 120-130.

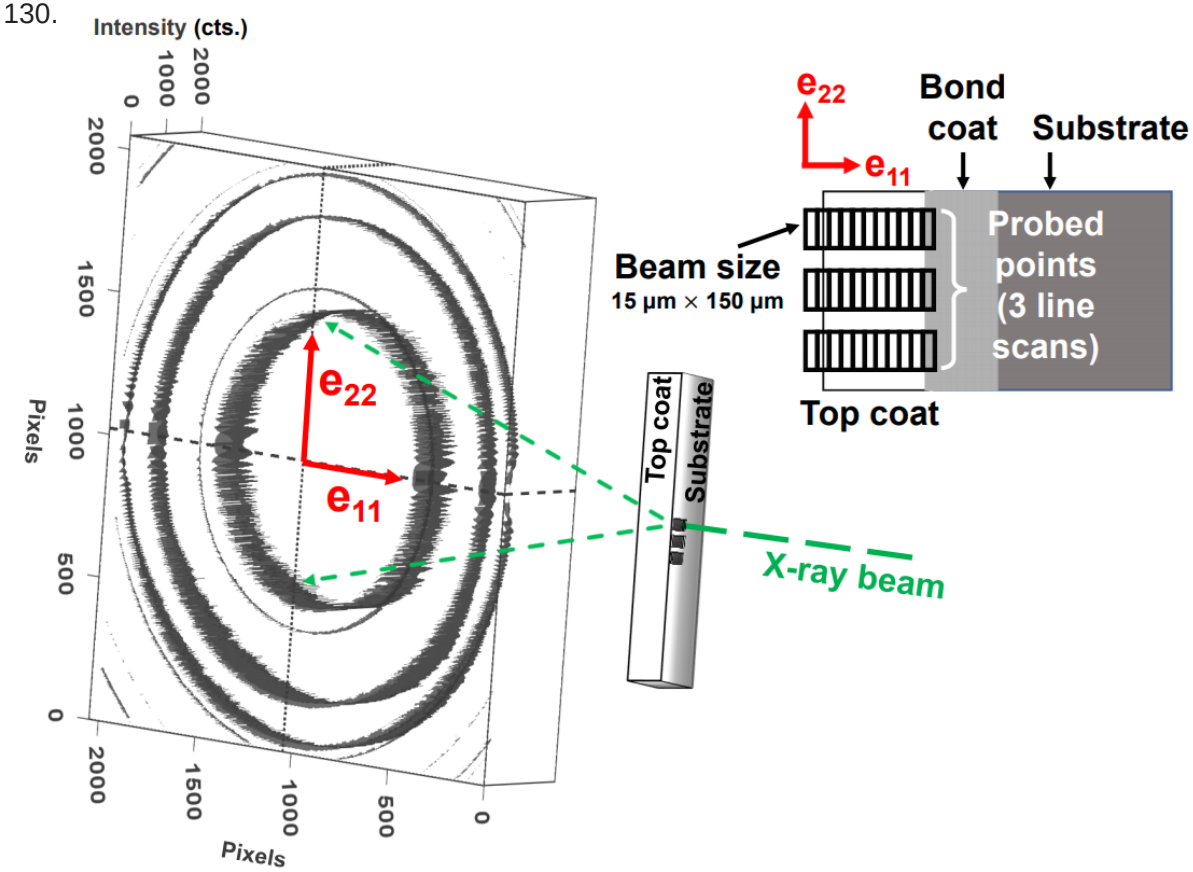

- Deviatoric strain which represents non-hydrostatic microdeformation can be measured by quantifying the eccentricity of the Debye-Scherrer rings.

Bragg's law: $n\lambda = 2dsin\theta$

Tetragonal: $\frac{1}{d^2} = \frac{h^2+k^2}{a^2} + \frac{l^2}{c^2}$

Sample-to-detector distance	178 cm
X-ray beam energy	71 keV
X-ray beam size	15 μm × 150 μm
Exposure time	300 ms
Step size (resolution)	15 μm

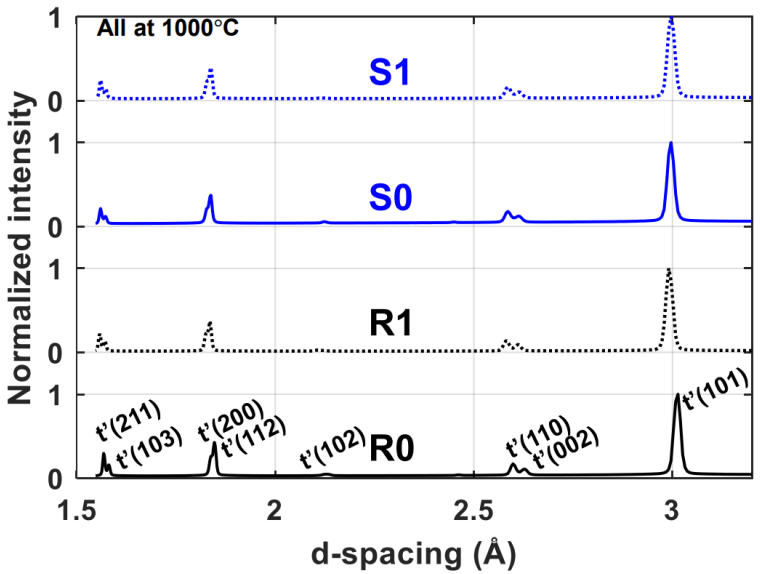

High temperature setup for *in-situ* characterization of TBCs at the synchrotron beamline

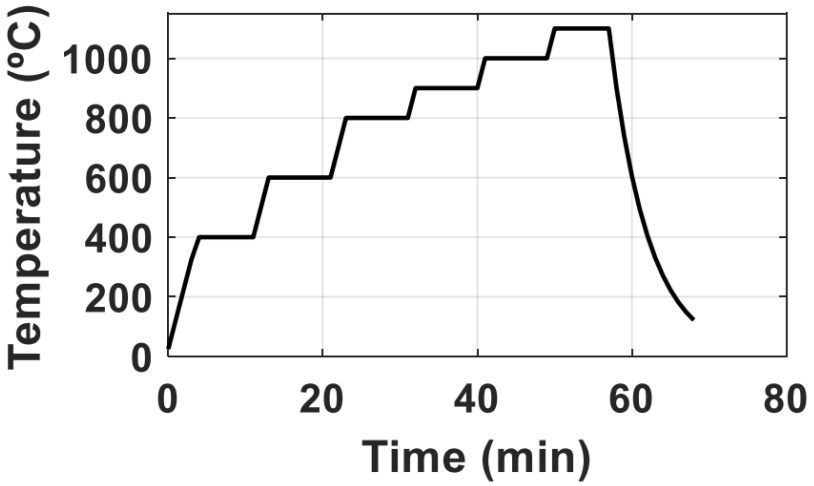

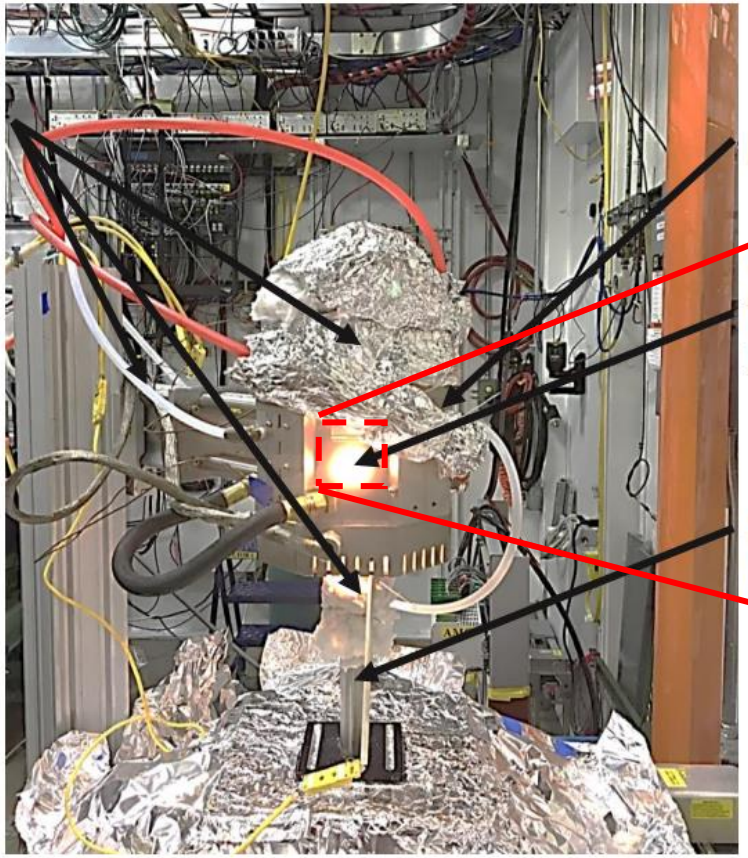

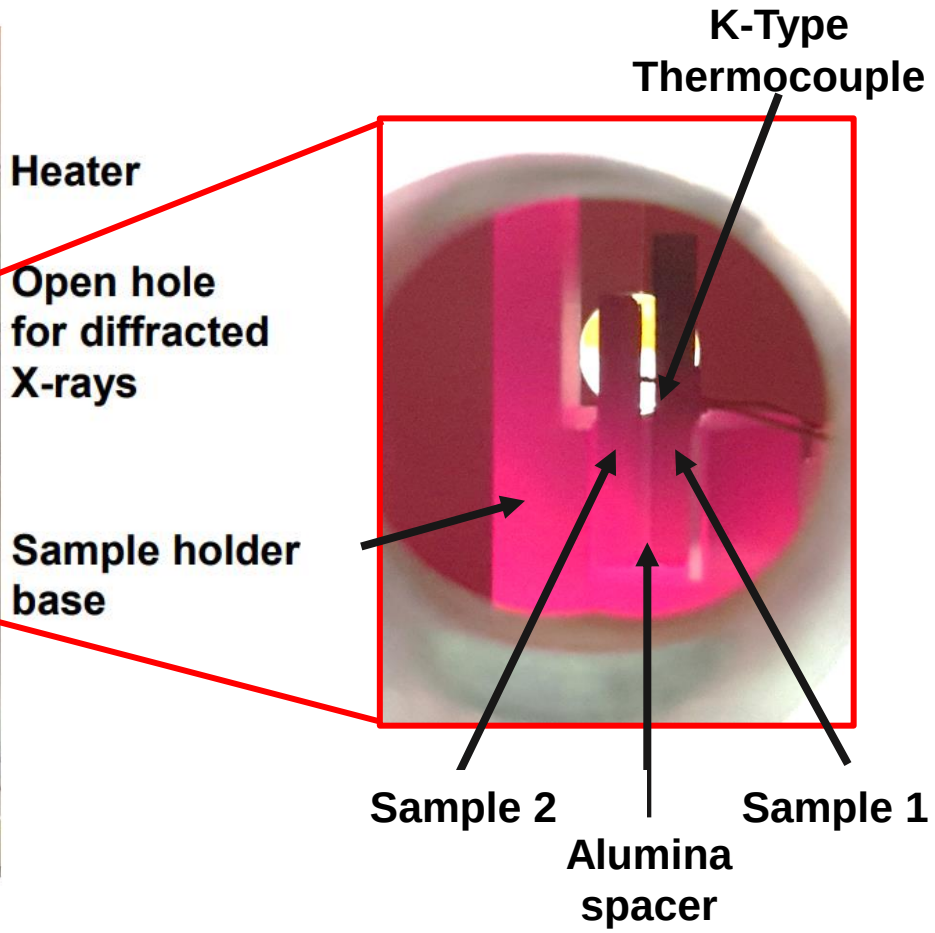

- 200°C/min ramps, 6-min holds
- 1 min hold for isothermal state in the top coats then data acquisition
- 5 min for data acquisition (0.3 s exposure per point)

Fouliard Ph.D. dissertation

Deviatoric strain vs. azimuth on major diffraction rings

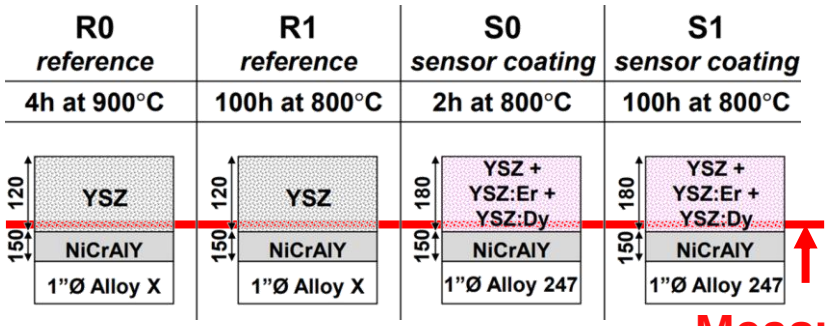

- Room temperature measurements
- The thermal aging (100h at 800˚C) resulted in TGO growth and compressive in-plane strain
- The strain magnitude remains comparable overall between reference (R) and sensor (S) coatings

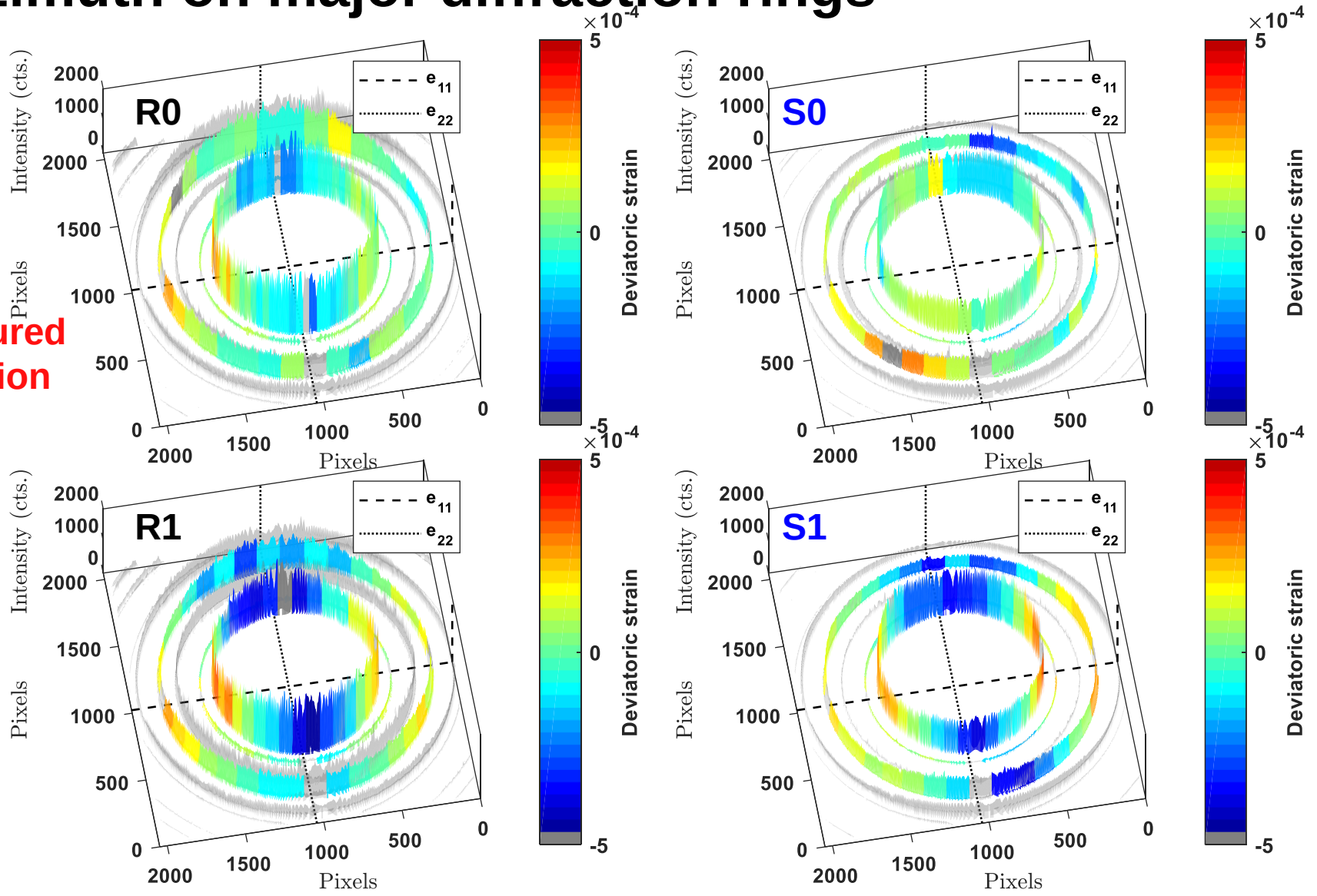

- We look here at the deviatoric strain measured for peaks (112) and (110) in addition of main analysis peak (101)

Deviatoric strain vs. coating depth using t’-(101)

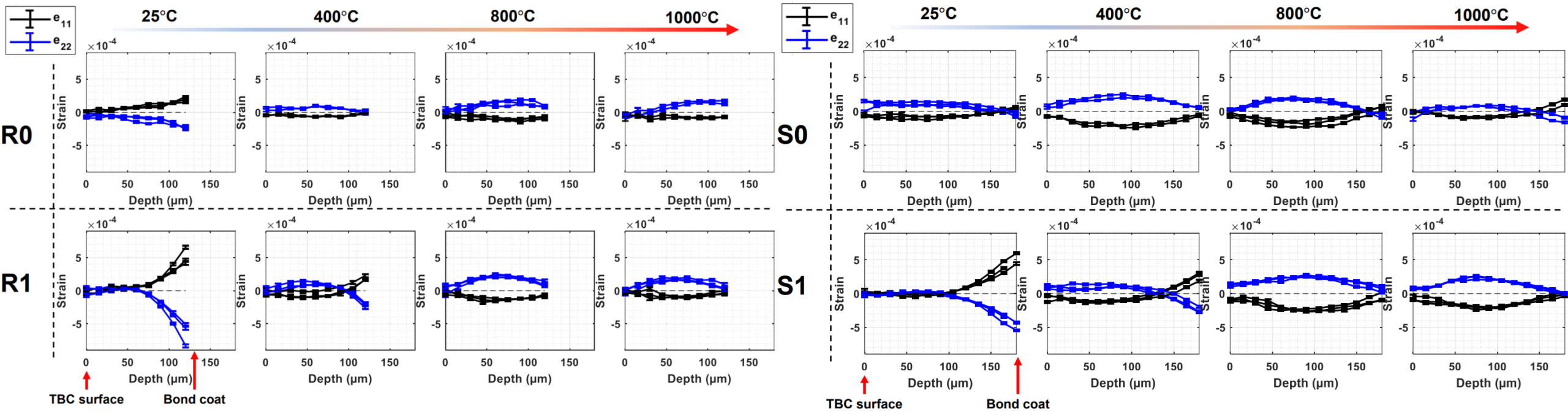

- Strains were measured with a depth resolution of 15 μm and 3 scans were performed for each coating and at each temperature hold to solidify results and to be able to statistically compare strain results
- e22 (in blue on the plots) is the in-plane (along the coating surface) strain, which gets compressive closer to the bond coat after thermal aging and this strain shows particularly at room temperature – generating coating fatigue under cyclic operation
- Strains are globally similar between R0 and S0 and R1 and S1, with low strain at top coat - bond coat interface, which is promising for the safe use of sensor coatings as they seem to possess comparable response under representative environments

Calculation of in-plane stress for coating comparison

$$\sigma_{22} = \frac{1}{\frac{1}{2}s_2}\left[\varepsilon_{22} - \frac{s_1}{\frac{1}{2}s_2 + 3s_1}(\varepsilon_{11} + \varepsilon_{22} + \varepsilon_{33})\right]$$

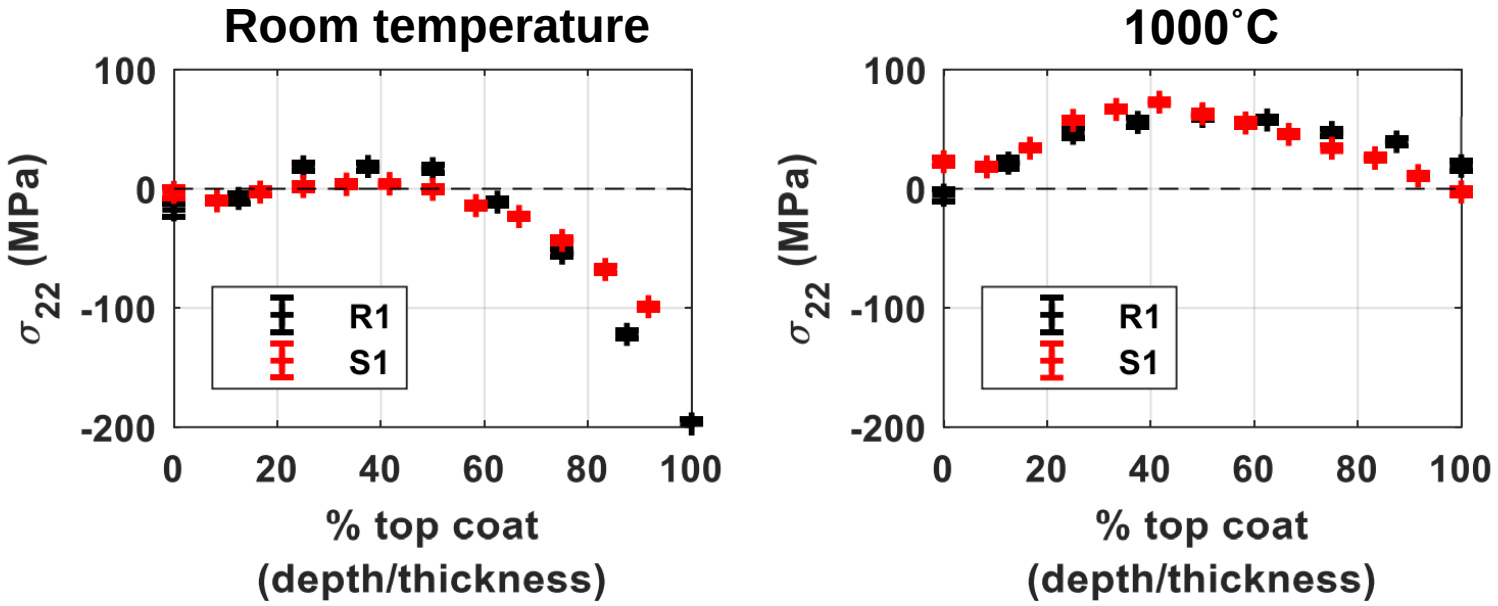

R1 *reference*	S1 *sensor coating*
100h at 800°C	100h at 800°C
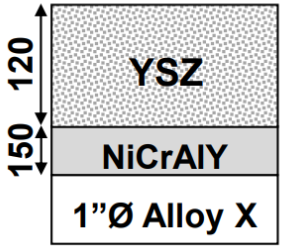	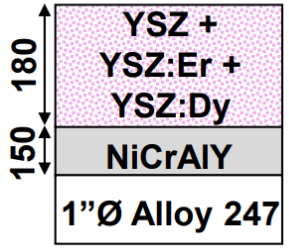

- σ_{22} calculated for coatings in operational conditions (here measured either at room temperature or at 1000˚C) remains similar in sensor coatings and in state-of-the-art (reference) coatings